

Old Dominion University

ODU Digital Commons

Electrical & Computer Engineering Theses &
Dissertations

Electrical & Computer Engineering

Fall 2006

Excimer UV Radiation from a Cylindrical Dielectric Barrier Discharge

Sudhakar Reddy Alla
Old Dominion University

Follow this and additional works at: https://digitalcommons.odu.edu/ece_etds



Part of the [Electrical and Computer Engineering Commons](#)

Recommended Citation

Alla, Sudhakar R.. "Excimer UV Radiation from a Cylindrical Dielectric Barrier Discharge" (2006). Master of Science (MS), Thesis, Electrical & Computer Engineering, Old Dominion University, DOI: 10.25777/k2rp-j933

https://digitalcommons.odu.edu/ece_etds/264

This Thesis is brought to you for free and open access by the Electrical & Computer Engineering at ODU Digital Commons. It has been accepted for inclusion in Electrical & Computer Engineering Theses & Dissertations by an authorized administrator of ODU Digital Commons. For more information, please contact digitalcommons@odu.edu.

**EXCIMER UV RADIATION FROM A CYLINDRICAL
DIELECTRIC BARRIER DISCHARGE**

by

Sudhakar Reddy Alla
B.Tech. May 2004, JNTU, Anantapur, AP, India.

A Thesis Submitted to the Faculty of
Old Dominion University in Partial Fulfillment of the
Requirements for the Degree of

MASTER OF SCIENCE

ELECTRICAL ENGINEERING

OLD DOMINION UNIVERSITY
December 2006

Approved by:

Mounir Laroussi (Director)

Sacharia Albin (Member)

Amin N. Dharamsi (Member)

ABSTRACT

EXCIMER UV RADIATION FROM A CYLINDRICAL DIELECTRIC BARRIER DISCHARGE

Sudhakar Reddy Alla
Old Dominion University, 2006
Director: Dr. Mounir Laroussi

Excimer lamps are intense non-coherent radiation sources, which emit UV or VUV radiation in a narrow wavelength range. The operation of these excimer lamps depends on the decomposition of excimers that are created in various non-equilibrium discharge plasmas. Excimer lamps mainly use rare gases or rare gas halides as the excimers formed by them emit radiation either in the UV or VUV region. This was confirmed in this work by observing the spectrum of the discharge in neon, krypton and chlorine gas mixture formed in a cylindrical dielectric barrier discharge (C-DBD). C-DBD's, which are non-equilibrium discharges, are used to generate excimer radiation as they can provide high-energy electrons and operate at high pressures that are required for the formation of excimers. The discharge in Ne/Kr/Cl₂ gas mixture is shown to be an efficient UV source in the wavelength range of 200 to 280 nm with strong emission bands centered around 200 nm (Cl₂^{**}), 222 nm (KrCl^{*}) and 258 nm (Cl₂^{*}).

The dependence of the intensity of UV radiation on different operating parameters, pressure in the discharge, voltage and frequency of the input signal and discharge tube diameter, is studied using a spectrometer and a UV calibrated photometer. It is shown that the maximum UV radiation intensity is achieved at a pressure of 250 torr and frequency of 18 kHz. The UV radiation intensity is found to be an increasing function of the other two operating parameters: input voltage and discharge tube

diameter. The effect of pressure, discharge tube diameter, input voltage and frequency on the electrical power consumed by the lamp is also studied. It is shown that the pressure in the discharge doesn't affect the power consumed by the lamp. But an increase in either discharge tube diameter or input voltage or frequency showed an increase in power consumption. Conversion efficiency of the lamp varied depending on pressure in the discharge and power consumed by the lamp. Efficiencies as high as 1.5% can be achieved under optimal conditions. This low cost excimer lamp can be used in applications like surface modification and water treatment.

ACKNOWLEDGMENTS

I would like to thank my advisor, Dr. Mounir Laroussi for his guidance and continuous support throughout this research and graduate study. His original ideas, experience and knowledge in the field have helped me to bring this work to a conclusion. I thank him for his encouragement and praise and for his belief in me. It has been an honor and a privilege to work with him. I also thank him for funding me with a Graduate Research Assistantship during this work. This work was partly funded by the Air Force Office of Scientific Research (AFOSR). I would like to thank AFOSR for that.

I would also like to thank Dr. A. Dharamsi and Dr. S. Albin for agreeing to serve on my committee. Special thanks are due to Dr. Xinpei Lu for his continuous help and valuable information during the course of this work. I also would like to thank Dr. Tamer, friends and colleagues for their encouragement during my study.

Finally, I would like to thank my parents, Venkateswara Reddy and Vijaya Lakshmi for their love and support. They are the main source of motivation for me. I would not have been who I am today with out their endless love and the sacrifices they made.

TABLE OF CONTENT

	Page
LIST OF TABLES.....	vii
LIST OF FIGURES.....	viii
CHAPTER	
I) INTRODUCTION.....	1
Excimers.....	2
Excimer generation mechanisms	2
II) EXCIMER FORMATION.....	14
Excimer Lamps.....	14
Excimer Formation.....	17
Rare gas excimers.....	19
Rare gas halide excimers.....	22
Discharge in Neon, Krypton and Chlorine gas mixture.....	26
Applications of excimer lamps.....	29
III) EXPERIMENTAL SET-UP AND PROCEDURES.....	32
Experimental set-up.....	32
Electrode Configuration.....	32
Vacuum System.....	34
Spectrometer set-up.....	36
Measurements.....	37
Power Calculations.....	37
Efficiency Calculations.....	39

IV) RESULTS AND DISCUSSION.....	41
Power Measurements.....	41
Emission spectroscopy.....	46
Spectral Measurements.....	48
Effect of Pressure.....	48
Effect of Voltage.....	52
Effect of Frequency.....	52
Effect of Discharge tube diameter.....	56
Power density Measurements.....	56
Effect of Pressure.....	58
Effect of Voltage.....	58
Effect of Frequency.....	61
Effect of Discharge tube diameter.....	61
Efficiency Measurements.....	61
V) SUMMARY.....	67
REFERENCES.....	70
VITA.....	73

LIST OF TABLES

Table	Page
2.1. Wavelengths of the resonance line and the three continua for the rare gases Ar, Kr, Xe	22
2.2. Wavelengths at which RgX* emit radiation for different transitions.....	24

LIST OF FIGURES

Figure	Page
1.1 Dielectric Barrier Discharge Configurations	4
1.2 Dependence of the mean electron energy on the product pd in xenon.....	6
1.3 End-on View of microdischarges.....	7
1.4 The life cycle of one microdischarge.....	9
1.5 General model of dielectric barrier discharges.....	10
1.6 Dielectric barrier discharge excimer lamp configurations.....	13
2.1 Emission spectra of different silent discharge excimer lamps.....	15
2.2 Planar excimer UV source.....	16
2.3 Cylindrical excimer UV source.....	16
2.4 Selection of wavelengths that can be generated in silent discharges.....	18
2.5 Potential energy diagram of xenon and corresponding excimer emission.....	21
2.6 Potential energy diagram for rare gas halide excimers.....	25
2.7 Potential energy diagram of KrCl.....	28
2.8 Dissociation energies of several chemical bands and wavelengths of different excimer molecules.....	30
3.1 Experimental set-up.....	33
3.2 Photograph of the actual system.....	33
3.3 Electrode configuration.....	35
3.4 Photograph of the discharge tube.....	35
3.5 Internal spectrometer set-up.....	38
3.6 Equivalent electrical circuit of the discharge.....	38

3.7 Experimental setup for measuring UV power density.....	40
4.1 Variation in Charge and Voltage with respect to Time: Discharge in Ne/Kr/Cl ₂ gas mixture at V = 8 kV, f = 18 kHz, p = 150 torr.	43
4.2 Q-V graph (Lissajous figure) of the Discharge at V = 8 kV, f = 18 kHz, p = 150 torr.....	43
4.3 Power consumed by the lamp as a function of Voltage at a frequency of 18 kHz.....	44
4.4 Power consumed by the lamp as a function of Frequency at a voltage of 14 kV and pressure of 100 torr.....	45
4.5 Power consumed by the lamp as a function of Pressure at a frequency of 18 kHz and voltage of 16 kV.....	45
4.6 Emission spectrum of the Discharge in Ne/Kr/Cl ₂ gas mixture at V = 16 kV, f = 18 kHz, p = 250 torr.....	47
4.7 Photograph of the Discharge at V = 16 kV, f = 18 kHz, p = 250 torr.....	47
4.8 Intensity of KrCl [*] and Cl ₂ [*] emission bands as a function of Pressure at V = 16 kV, f = 18 kHz.....	49
4.9 Intensity of KrCl [*] and Kr ₂ Cl [*] emission bands as a function of Pressure at V = 16 kV, f = 18 kHz.....	50
4.10 Emission spectrum of the Discharge in Ne/Kr/Cl ₂ gas mixture at pressures of 250 and 450 torr: V = 16 kV, f = 18 kHz.....	51
4.11 Intensity of KrCl [*] and Cl ₂ [*] emission bands as a function of Voltage at p = 25 torr, f = 3 kHz.....	53

4.12 Intensity of KrCl^* and Cl_2^* emission bands as a function of Frequency at $p = 25$ torr, $V = 16$ kV.	54
4.13 Emission spectrum of the Discharge in Ne/Kr/ Cl_2 gas mixture at frequencies of 3, 18, 23 and 25 kHz: $V = 16$ kV, $p = 25$ torr.....	55
4.14 Emission spectrum of the Discharge in Ne/Kr/ Cl_2 gas mixture for two different discharge tube diameters of 0.25 and 0.5 inch	57
4.15 Power density of the discharge as a function of Pressure at $V = 16$ kV, $f = 18$ kHz.....	59
4.16 Power density of the discharge as a function of Voltage at $f = 18$ kHz, $p = 100$ torr.....	60
4.17 Power density of the discharge as a function of Frequency at $V = 16$ kV, $p = 100$ torr.....	62
4.18 Power density of the discharge as a function of Pressure at $V = 16$ kV, $f = 18$ kHz for discharge tube diameters of 0.25 and 0.5 inch.....	63
4.19 Efficiency as a function of Pressure for discharge tube diameters of 0.25 and 0.5 inch: $f = 18$ kHz, $V = 16$ kV.....	65
4.20 Efficiency as a function of Power for discharge tube diameters of 0.25 and 0.5 inch: $f = 18$ kHz, $p = 250$ torr.....	66

CHAPTER I

INTRODUCTION

Plasmas are a collection of electrons, ions, neutrals and fields that exhibit collective effects. Plasmas are the 4th state of matter and they comprise more than 99% of the visible universe. Plasmas are formed when electrons are stripped from the atoms and converted to ions. Plasma temperatures and densities vary in a wide range. The temperatures of plasmas vary from absolute zero to 100 keV [1]. Since plasmas contain electrons and ions, they can be good conductors of electricity and can respond to electromagnetic fields. Plasmas can be efficient sources of radiation and thus can be used in many applications where such radiation is needed. Plasmas have a wide range of applications and are used in fluorescent lamps, semiconductor processing, high power microwave sources, flat panel displays, gas lasers, radio transmission around the world, pulsed power switches and sterilization of media.

Plasmas can be classified into two types based on the temperature of the electrons and that of the heavy species (ions and neutrals). The first type is the thermal or equilibrium plasma. In equilibrium plasmas, the temperature or energy level of the electrons is equal to that of ions and neutrals. These thermal plasmas are used in welding, arc furnace technology and plasma spraying. The other type is the non-equilibrium plasma. They are also referred to as two-temperature plasmas or cold plasmas. In these types of plasmas, the temperature or energy level of the electrons will be much higher than that of the ions and neutrals. Such plasmas have found a large number of applications in plasma etching, plasma assisted chemical vapor deposition and in excimer sources.

1.1 Excimers

Excimers (excited dimers) are weakly bound excited diatomic molecules. Under normal conditions, excimers do not possess a stable molecular ground state. Typical examples of excimers are rare gas excimers such as Ar_2^* , Kr_2^* , Xe_2^* or rare gas halide excimers such as KrCl^* , ArF^* , XeCl^* . Actually the rare gas halide excimers are not excited dimers but they are excited complexes (exciplex) and so must be called exciplex molecules. But most of the researchers refer to them as excimers. The same convention is followed throughout this document and hereafter the excited rare gas halide molecules are referred to as rare gas halide excimers. A comprehensive review of excimers is given in the book "Excimer lasers" edited by Ch.K. Rhodes [2]. Excimers are highly unstable and so will disintegrate quickly giving up the extra energy in the form of photons. The lifetime of excimers is very short, in the order of a few nanoseconds. The excimer emission from rare gas or rare gas halides is either in the UV or VUV region. The lamps that use rare gas or rare gas halides to generate UV and VUV radiation by the above effect are called excimer lamps, or excilamps. The operation of these excimer lamps depends on the decomposition of the excimers, which are created in various non-equilibrium discharge plasmas. The devices used for the generation of excimers, particularly the dielectric barrier discharges are discussed in the following section.

1.2 Excimer Generation Mechanisms

Non-equilibrium discharges are mostly used to create excimers as they can provide high-energy electrons and can operate at high pressures that are required for the formation of excimers. Different types of discharges have been used for the generation of excimers, which include microwave discharges [3], glow discharges [4,5], microhollow

cathode discharges [6,7] and supersonic discharges [8]. The most widely used discharge is the dielectric barrier discharge (DBD) [9-18]. Dielectric barrier discharges are non-equilibrium electrical discharges that can be operated at high pressures, i.e. around atmospheric pressure. In dielectric barrier discharge, the electron density and the average electron energy can be controlled by the operating parameters. In addition to the above advantages, it has great flexibility with respect to geometrical shapes and size of the discharge.

Dielectric Barrier Discharges, also known as silent discharges, are a special type of gaseous discharges that self limit their current flow. They can operate at high voltages and relatively high pressures of up to one atmosphere. The typical configurations used in dielectric barrier discharges are shown in Fig. 1.1 [19]. The dielectric barrier discharge system has a dielectric layer that covers one or both of the electrodes. The mostly used materials for the dielectric barrier are glass, ceramics and quartz. In special cases polymer coatings are also used. The dielectric barrier is an insulator and so it cannot pass a dc current. This is the reason why dielectric barrier discharges are operated with alternating voltages. The discharge appears in the gap between the electrodes when an ac voltage is applied to the electrodes. At high frequencies the current limitation by the dielectric becomes less effective. Therefore, the dielectric barrier discharges are normally operated between line frequency and few MHz range.

In dielectric barrier discharges, most of the plasma parameters can be controlled by external means. By changing the pressure in the discharge and the electrode spacing, the average energy of the electrons (T_e) can be controlled. By changing average energy of

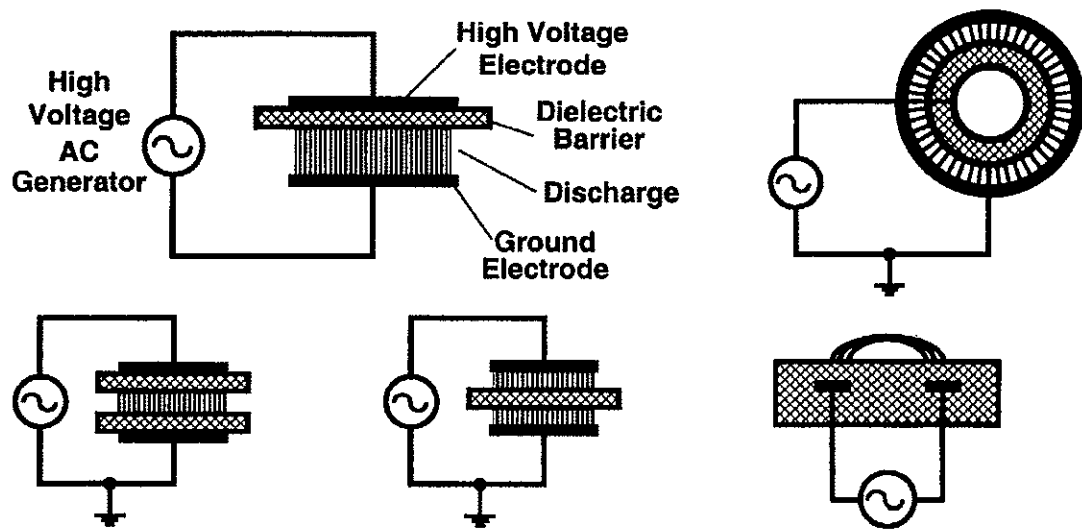


Fig. 1.1. Dielectric Barrier Discharge Configurations [19].

the electrons one can optimize the production of various desired plasma species. For example, high-energy electrons can be used for the formation of excimers. Fig. 1.2 [20] shows the dependence of mean electron energy on the gas density times the inter-electrode gap distance (nd) in xenon gas.

The breakdown occurs in the discharge when the field in the gap exceeds the Paschen minimum value. The Paschen voltage is the minimum voltage required to initiate a breakdown. The Paschen value can be obtained by dividing Paschen voltage with the product nd . When the voltage is applied across the discharge gap, the electrons start moving from the cathode towards the anode. The free electrons on their way to the anode collide with the gas atoms or molecules and create new electrons and ions, which initiate an avalanche process. When the electric field in the gap is high enough, breakdown occurs. There are two types of breakdowns, which can be classified based on the product of gas density and the gap distance (nd). When the value of nd is low (near Paschen minimum value), the breakdown occurs with negligible space charge in the gap. This breakdown is a feedback process between the avalanches and the secondary electrons that are emitted from the cathode. This is a slow process and takes a number of avalanches to complete it. This breakdown is known as Townsend breakdown. The Townsend breakdown depends on the nature of the cathode material. The other type of breakdown occurs when the value of nd is high. This type of breakdown generates a considerable space charge in the discharge gap.

The breakdown results in a formation of large number of microdischarges. The microdischarges are single transit discharges. Fig. 1.3 [21] shows the end on view of microdischarges in air at atmospheric pressure. The microdischarges propagate under the

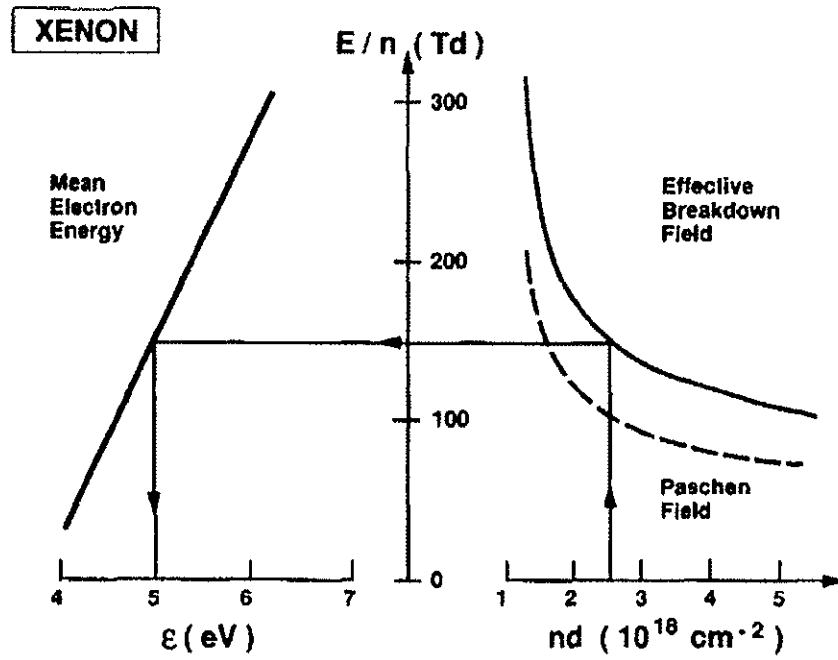


Fig. 1.2. Dependence of the mean electron energy on the product nd in xenon gas: n is gas density and d is the distance between electrodes [20].

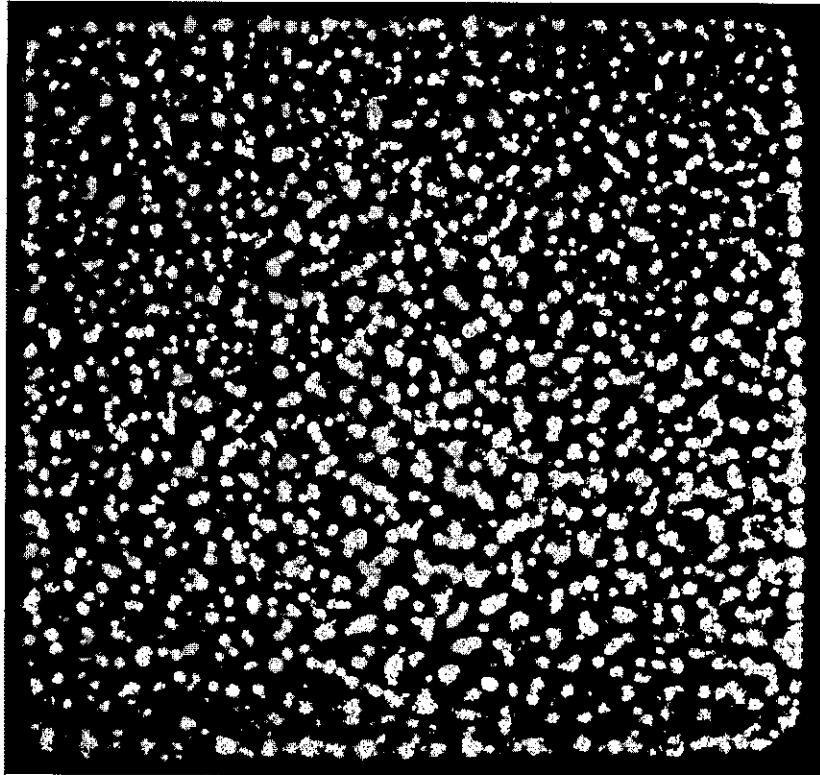


Fig. 1.3. End-on View of microdischarges [21].

influence of their own field. This means they are independent of all the processes that are going around them. These discharges are inhomogeneous. However, under special conditions homogenous discharges can also be obtained. The microdischarges live only for a short duration of the order of 100 ns. The radius of the microdischarge channel is of the order of 100 μm . The microdischarges are weakly ionized plasma channels where most of the current flows. The typical current densities in a microdischarge are 100-1000 A/cm^2 [21]. The thickness of the dielectric barrier, the gap spacing, and also gas properties can influence the amount of charge that is carried by an individual microdischarge.

To understand the concept of electrical breakdown one has to understand the internal conditions in the microdischarges. The life cycle of one microdischarge is shown in the Fig. 1.4 [20]. This figure shows that the initial electrons excite the gas species A after some time delay. When the excited electrons collide with the species A, some of the atoms get ionized, while some of atoms or molecules absorb the kinetic energy of the excited electrons and transform to an excited species (A^*). The excited species A^* react and form a new species B.

The general model of the dielectric barrier discharges is shown in the Fig. 1.5 [19]. Here, four processes can be identified in the model of a dielectric barrier discharge: a) the application of an electric field; b) formation of fast electrons and ions; c) formation of the excited species and d) initiation of chemical reactions. Different combinations of the pressure, temperature, discharge gap, gas mixture, and the dielectric barrier result in different chemical reactions in the plasma. Depending on the applications, different reactions will be of importance. The conditions leading to the formation of excimers are

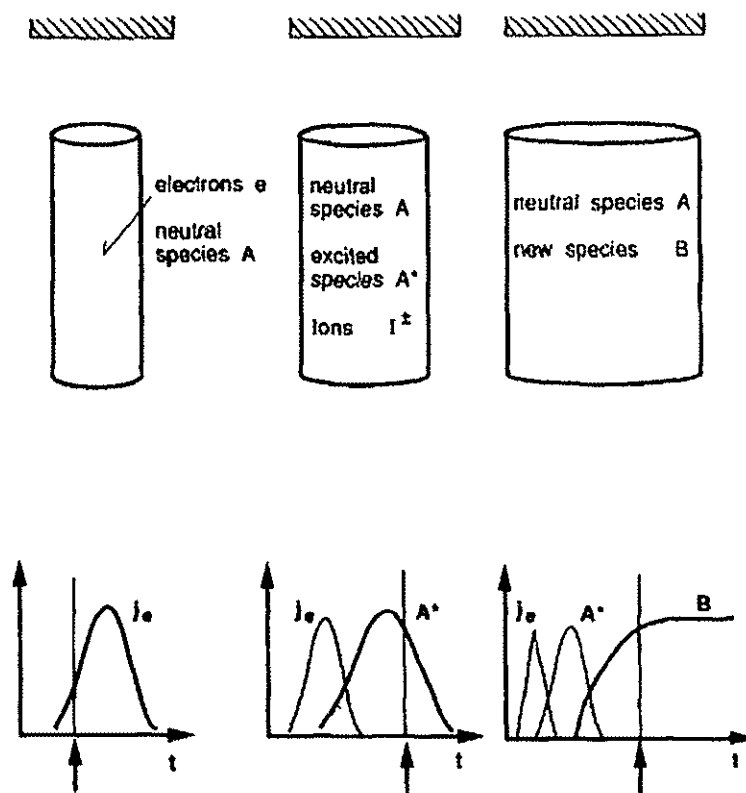


Fig. 1.4. The life cycle of one microdischarge [20].

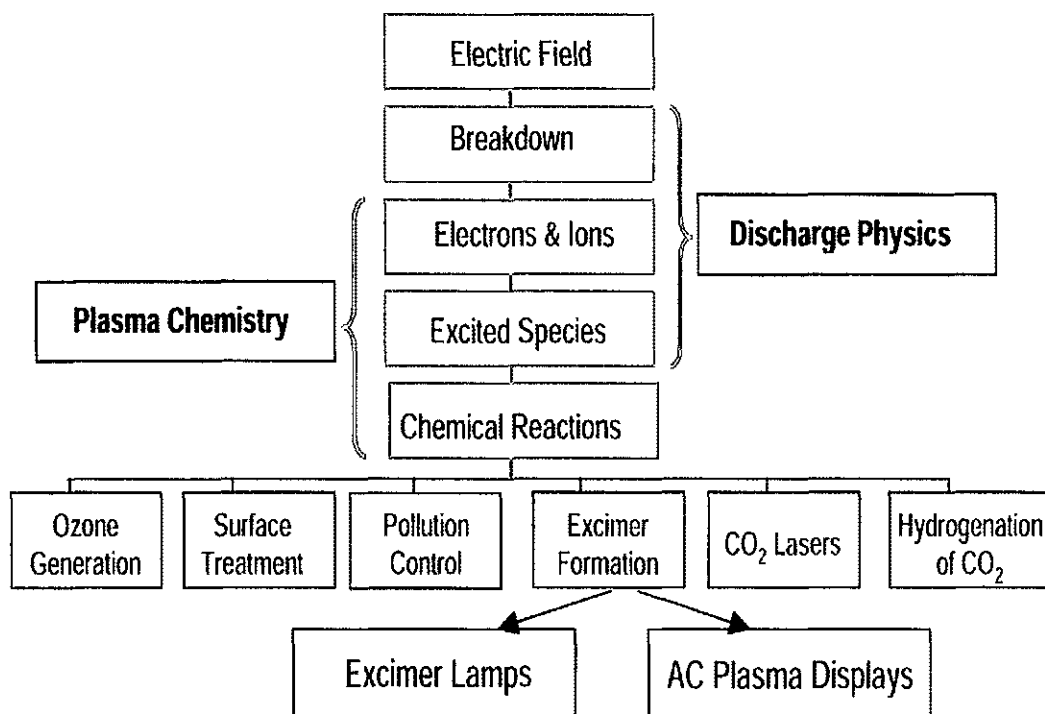


Fig. 1.5. General model of dielectric barrier discharges [19].

used in excimer lamps. Different dielectric barrier discharge configurations used in excimer lamps are shown in Fig. 1.6 [22]. In addition to their use in excimer lamps, dielectric barrier discharges are suitable for a wide range of applications such as ozone generation, surface treatment and modification, coating, pollution control, sterilization, high power CO₂ lasers, fluorescent lamps and plasma display panels.

In most of the configurations discussed above an outer electrode usually made of wire mesh or perforated metal is used. This electrode generally occupies a sizable portion of the total area through which the UV radiation is to escape to the outside. Therefore, a non-negligible percentage of the UV emitted is blocked by this electrode. To overcome this problem, Laroussi [23,24] proposed a new device configuration. In this design, the electrodes are formed by two thin metallic rings wrapped around the outside wall of a hollow, cylindrical dielectric tube. The hollow tube can be filled by the desired gas or gas mixture and then sealed. The ring electrodes are placed at a distance from each other and take up a negligible area of the outside wall. This way, the UV generated by the discharge inside the dielectric tube propagates outside practically unimpeded and therefore non-attenuated. An important advantage of having both electrodes placed on the outside of the tube is the fact that they do not come in contact with the discharge. Therefore, no contamination of the plasma by the electrodes occurs. Electrode contamination reduces UV generation, and limits the lamp lifetime. The work in this thesis is based on the configuration proposed by Laroussi.

This thesis is organized in five chapters including the introduction chapter. The introduction chapter gives an idea about excimers and different excimer generation mechanisms. The dielectric barrier discharges are discussed in detail, as they are similar

to the configuration that we used in our experiments. Chapter 2 discusses excimer lamps and their applications. The formation of rare gas and rare gas halide excimers are also discussed. Chapter 3 presents the experimental setup and procedures. Here, the method for calculating electrical power consumed by the discharge and internal efficiency of the lamp are explained. The results that are obtained using optical spectroscopy and photometry are covered in chapter 4. Finally, the summary of the main results obtained in this work is presented in chapter 5.

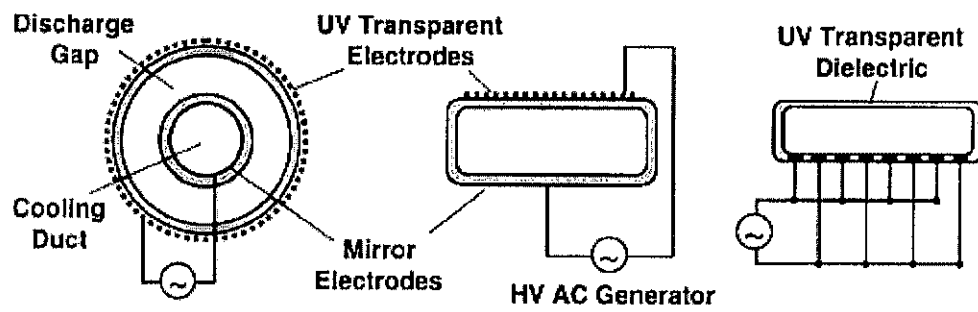


Fig. 1.6. Dielectric barrier discharge excimer lamp configurations [22].

CHAPTER II

EXCIMER FORMATION

2.1 Excimer lamps

Excimer lamps are intense non-coherent radiation sources, which emit UV or VUV radiation in a narrow wavelength range. The emission spectra of different silent discharge excimer lamps are shown in Fig. 2.1 [25]. These types of sources, which can emit high intensities of UV/VUV radiation at a narrow wavelength range, are required for many applications such as UV curing, UV lithography, UV sterilization, surface modification and photodecomposition [26-28]. Both plane (Fig. 2.2 [9]) and cylindrical (Fig. 2.3 [9]) geometries can be used in excimer lamps.

The excimer UV and VUV radiations are considered for many applications because they are environmentally friendly and do not generate any harmful byproducts. Other than excimer lamps, there are many devices that can generate radiation in the UV or VUV spectral range. Examples are the mercury lamps, xenon lamps, and deuterium lamps. But the excimer lamps have an edge over the above-mentioned sources as the excimer lamps have high efficiency, narrow emission band, long lifetime, and relatively high radiation power density. Also excimer lamps do not use toxic materials like mercury making them environmentally friendly. The other advantage of excimer lamps is their lack of self-absorption of the emitted radiation because the excimers, which are responsible for the radiation, do not have stable ground states. In addition to the above advantages excimer lamps have great flexibility with respect to geometrical shape and size. These are the reasons for the preference of excimer lamps over other UV/VUV sources.

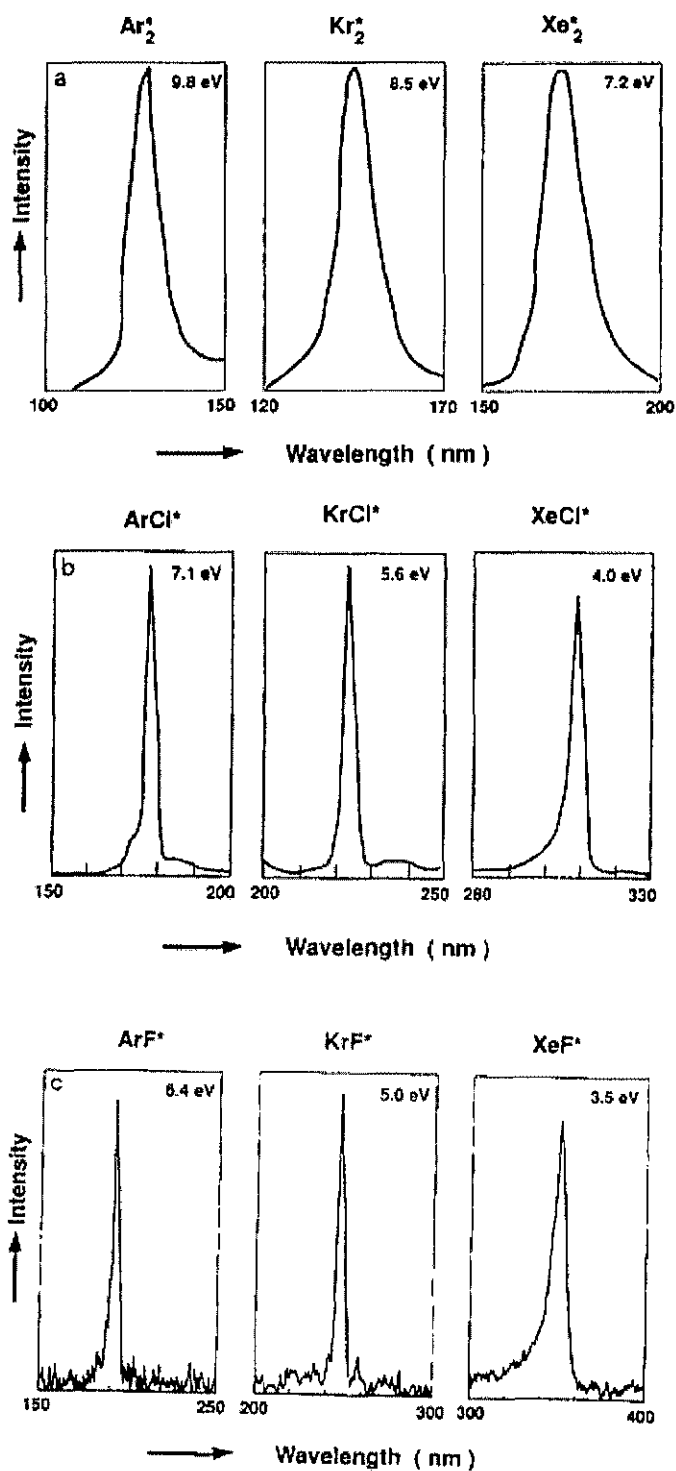


Fig. 2.1. Emission spectra of different silent discharge excimer lamps. Values in the corner represent energy of photons that are emitted by respective excimers shown on top [25].

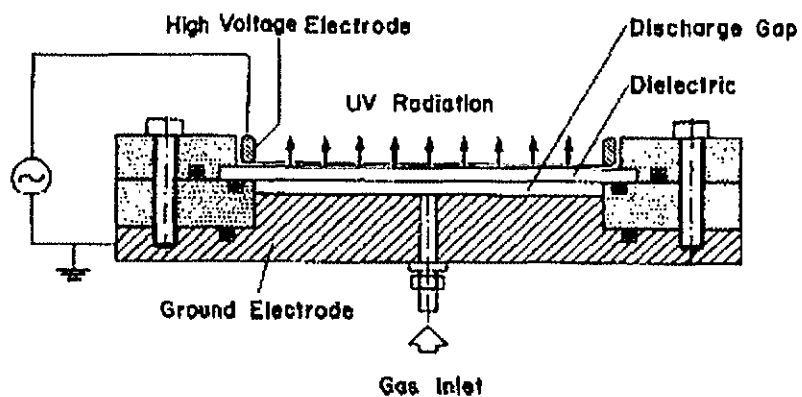


Fig. 2.2. Planar excimer UV source [9].

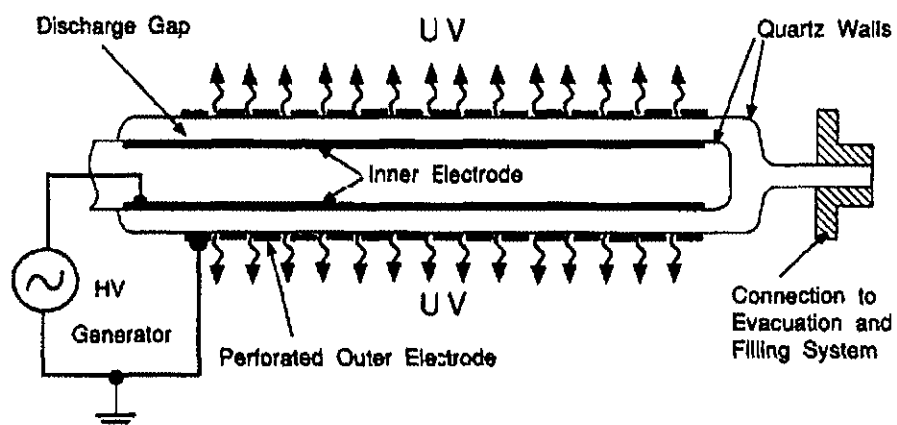


Fig. 2.3. Cylindrical excimer UV source [9].

There is one more type of source, excimer laser, which emits radiation in UV and VUV spectral range. Excimer lasers generate monochromatic radiation and are presently the highest-powered sources in the above-mentioned range. Excimer lamps have an advantage over lasers regarding the choice of wavelengths. Excimer lasers provide only a limited number of wavelengths. But with excimer lamps there are more than 20 different wavelengths at which radiation can be generated in the UV or VUV range. The selection of excimer wavelengths that can be generated in silent discharges is shown in Fig. 2.4 [25]. As excimer lamps are non-coherent radiation sources, they can be easily scaled to a large size. This helps to irradiate and treat large area surfaces easily. Finally, the main advantage of replacing lasers with the excimer lamp in large area processing is because of its low cost when compared with lasers.

The operation of excimer lamps depends on the decomposition of the excimers that are created in various non-equilibrium discharges. Non-equilibrium discharges are used to create excimers because they can provide high electron energies and can operate at high pressures that are required for the formation of excimers. Different rare gases or rare gas halides are used in excimer lamps to generate UV/VUV radiation at different wavelengths [10-14,29,30]. In the following sections the formation of excimers and the applications of excimer lamps are discussed.

2.2 Excimer formation

There are mainly two conditions that must be satisfied for efficient excimer formation. The first condition that must be satisfied is the presence of high-energy electrons in the discharge, whose energy must be high enough to excite the atoms in the

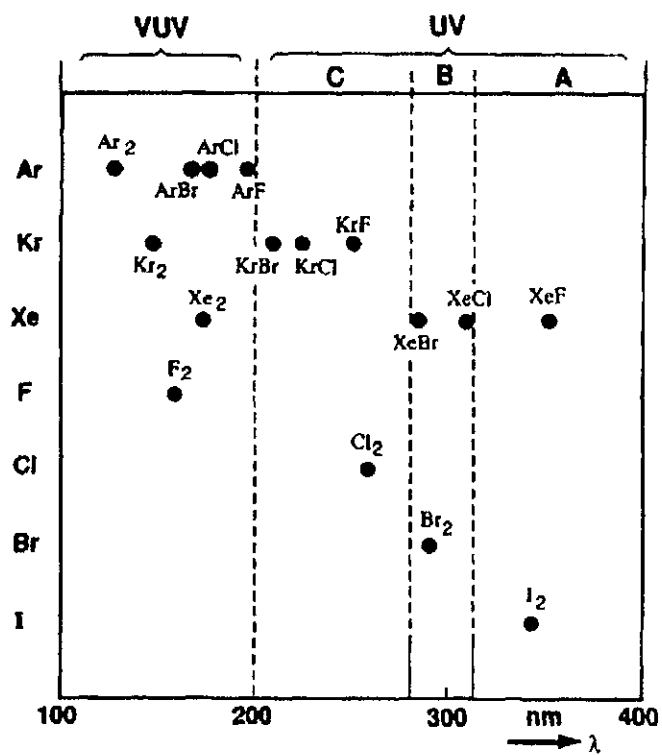


Fig. 2.4. Selection of wavelengths that can be generated in silent discharges [25].

ground state. Secondly the pressure in the discharge tube must be relatively high, near atmospheric pressure, to make the three body reactions that are responsible for the formation of excimers more favorable. Excimers are formed when the excited atom reacts with another atom in the presence of third atom. Typical examples of excimers are rare gas excimers such as Ar_2^* , Kr_2^* , Xe_2^* or rare gas halide excimers such as KrCl^* , ArF^* , XeCl^* . The reactions that involve the formation of rare gas excimers and rare gas halide excimers are complex and involve several ground state atomic and molecular species and large number of excited species. The formation of excimers can be divided into three major processes: a) ionization and excitation of atoms; b) formation of excimers; c) emission of radiation. All of these processes are discussed in detail in the following sections for both rare gas excimers and rare gas halide excimers.

2.2.1 Rare gas excimers

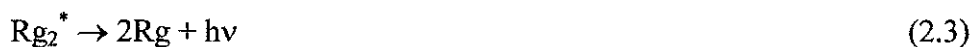
As mentioned above, the formation of excimer requires high pressures and high-energy electrons. The high-energy electrons can be generated either by a gas discharge or by an electron beam. These high-energy electrons present in the discharge will collide with the rare gas atoms and either ionize or excite them. Many researchers have extensively studied the physics of different processes to understand the formation of rare gas excimers and developed kinetic models [2,31,32]. Here, the main reactions that lead to the formation of rare gas excimers are discussed.



where Rg is a rare gas atom (e.g., Ar, Kr, Xe, etc.), Rg^* is the rare gas excited states, and e is the electron. At high pressures, the excited rare gas atom reacts with another rare gas atom in the presence of third atom and undergoes three-body collision according to:



where Rg_2^* is the rare gas excimer molecule. The three body collision and hence the formation of excimers is favored at high pressures. The rare gas excimer formed is highly unstable and so decomposes quickly into rare gas atoms giving out the extra energy in the form of UV or VUV radiation.



The UV or VUV radiation generated is a result of the transition of excimer from the excited state to the repulsive ground state. Depending on the pressure, the rare gas excimer will radiate in different ways. At low pressures, the excimers will radiate in the first continuum from higher vibrational levels to the repulsive ground state. The first continuum will result from the transition of excimer from $^3\text{P}_1 \rightarrow ^1\text{S}_0$ states. At high pressures, the excimers will radiate in the second continuum from lower vibrational levels to the repulsive ground state. The second continuum will result from the transition of excimer from $^3\text{P}_2 \rightarrow ^1\text{S}_0$ states. Both these transitions for xenon are shown in Fig. 2.5. [11]. There is also a resonance line that can be seen in the figure. The resonance line is present at very low pressures where the formation of excimers is less likely to happen. The resonant line emission occurs as a result of spontaneous emission of the excimer from the excited state to the ground state. The third continuum is because of the transition between Rg^{2+} to Rg states. The wavelength of the resonance line and the three continua for the three rare gases Ar, Kr, Xe are shown in the Table 2.1 [11,33]. It can be seen from the table that the rare gases emit at different wavelengths in the three continua and resonance line. So, by changing the pressure in the discharge tube the wavelength of the peak UV or VUV intensity can be varied.

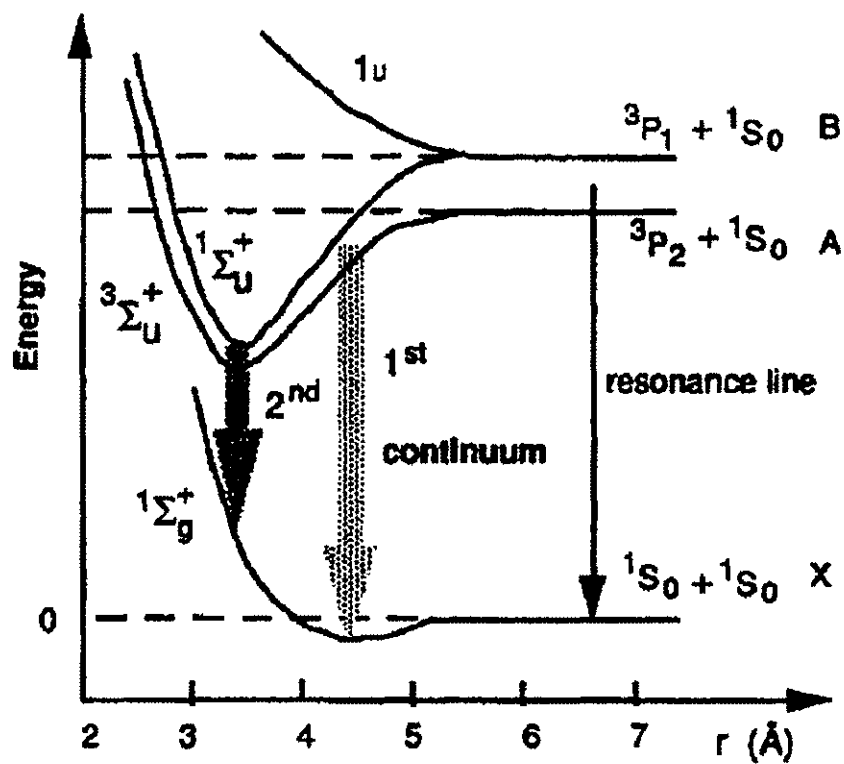


Fig. 2.5. Potential energy diagram of xenon and corresponding excimer emission [11].

Table 2.1. Wavelengths of the resonance line and the three continua for the rare gases Ar, Kr, Xe [11,33].

Rare gas	I / II Resonance line (nm)	I Continuum (nm)	II Continuum (nm)	III Continuum (nm)
Ar	106.4/104.8	110	126	188
Kr	123.6/116.5	125	146	220...270
Xe	146.96/129.56	150	172	300

2.2.2 Rare gas halide excimers

In addition to the rare gas excimers discussed above, there is one more class of excimers called rare gas halide excimers. The reaction mechanisms that lead to the formation of rare gas halide excimers are very complex. Here, only the main reactions that lead to the formation of rare gas halide excimers are discussed [12]. As discussed in the rare gas excimers section, the first step in the formation of excimers is the ionization and excitation of the atoms. The high-energy electrons present in the discharge collide with the atoms and will either ionize or excite them.



where Rg represents a rare gas atom (e.g., Ar, Kr, Xe, etc.) and X represents a halogen atom (e.g., F, Cl, Br, I). The halogen ion X^- is formed as a result of dissociative electron attachment to the halogen molecule X_2 . In the excited state, rare gas atoms will have one

electron in the outer most shell. So, the excited rare gas atoms behave like the alkali atoms and readily enter into reaction with the halogens to form RgX^* .



The type of reaction described by above equation (2.7) is called a harpooning reaction. A harpooning reaction is a reaction in which an atom transfers its loosely bound electron to another atom and forms an excited molecule. There is also one more reaction through which RgX^* excimers can be created. It is the three-body ion-ion recombination. The positive rare gas ion reacts with the negative halogen ion in the presence of a third body and forms RgX^* .



where M is the third collisional body. M can also be a buffer gas atom. The buffer gas is used to influence the electron energy distribution. One more reason for using the buffer gas is because of the cost of different rare gases. Most of the RgX^* excimers are created either by three-body ion-ion recombination or by harpooning reaction. Thus formed rare gas halide excimer is highly unstable and so quickly decomposes into atoms giving out the extra energy in the form of UV or VUV radiation.



A potential energy diagram for rare gas halide excimers is shown in Fig. 2.6 [12]. There are three possible excited states $B_{1/2}$, $C_{1/2}$, $D_{1/2}$, and three possible ground states $A_{1/2}$, $A_{3/2}$, $X_{1/2}$ for a rare gas halide excimer. The excimer transitions that can take place in rare-gas halides are shown in the figure. The intensity and spectral half width of the radiation for different transitions are different. The width of the lines in this figure indicates the relative intensities of the corresponding transitions. The different transitions

of RgX^* will emit UV or VUV radiation at different wavelengths. The wavelengths at which RgX^* emit radiation for different transitions and for different combinations of rare gases and halogens are given in Table 2.2 [12]. The emission spectrum of rare gas halide excimers consists of mainly a strong $B_{1/2} \rightarrow X_{1/2}$ transition band. The $B_{1/2} \rightarrow X_{1/2}$ transition is the strongest because the initial and final $p\sigma$ orbitals, which the electron occupies, have the largest overlap of any of the valence orbital [2]. Among all transitions, the $D_{1/2} \rightarrow X_{1/2}$ transition emits the radiation at short wavelengths. The intensity of $D_{1/2} \rightarrow X_{1/2}$ transition is much less than that of $B_{1/2} \rightarrow X_{1/2}$ transition. The $C_{3/2} \rightarrow A_{3/2}$, $B_{1/2} \rightarrow A_{1/2}$ transitions result in weak broadband emissions. At high pressures triatomic excimers (Rg_2X^*) can also be generated. These Rg_2X^* molecules are generated due to three body collisions between rare gas atoms and the excited rare gas halides.



Table 2.2. Wavelengths at which RgX^* emit radiation for different transitions [12].

Rg	X	RgX^* $D_{1/2} \rightarrow X_{1/2}$ (nm)	RgX^* $B_{1/2} \rightarrow X_{1/2}$ (nm)	RgX^* $C_{3/2} \rightarrow A_{3/2}$ (nm)	RgX^* $B_{1/2} \rightarrow A_{1/2}$ (nm)	Rg_2X^* (nm)
Ne	F	106	108	110	111	~ 145
Ar	F	185	193	203	204	290 ± 25
Ar	Cl		175		195	245 ± 15
Ar	Br		165	172	183	
Kr	F	220	248	275	272	400 ± 35
Kr	Cl	200	222	240	235	325 ± 15
Kr	Br		207	222	228	~ 318
Kr	I		190	195	225	
Xe	F	264	351	460	410	610 ± 65
Xe	Cl	236	308	345	340	450 ± 40
Xe	Br	221	282	300	325	440 ± 30
Xe	I	203	253	265	320	~ 375

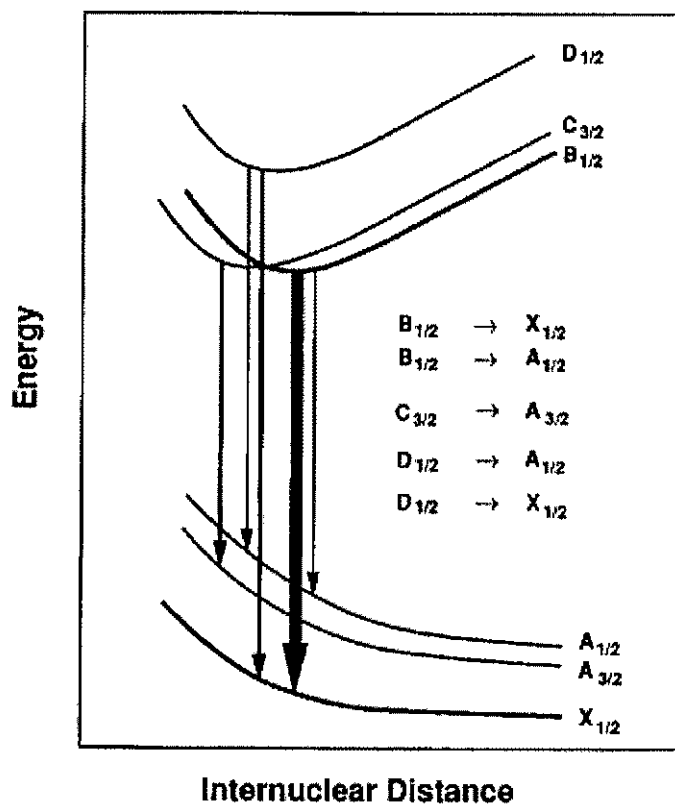


Fig. 2.6. Potential energy diagram for rare gas halide excimers [12].

2.2.3 Discharge in Neon, Krypton and Chlorine gas mixture

In our experiments, the discharge in neon/krypton/chlorine gas mixture is studied. KrCl^* , Kr_2Cl^* , Cl_2^* and Cl_2^{**} excimers formed as a result of the discharge in this gas mixture emit UV radiation in the 200 to 350nm wavelength range. In this section the various reactions that lead to the formation of these excimers are described. As discussed in the rare gas halide excimers section, the first step in the formation of excimers is the ionization and excitation of the atoms. The high-energy electrons present in the discharge collide with the atoms and will either ionize or excite them.



The characteristic time for Kr^+ ions to convert to Kr_2^+ dimers is 40 ns [34]. M in the reaction can be either neon (buffer gas) or krypton. In the excited state, rare gas atoms will have one electron in the outermost shell. So, the excited rare gas atom, Kr, behaves like an alkali atom and readily enters into reaction with the halogen molecule Cl_2 to form KrCl^* . Excited krypton chloride can also be formed when a positive krypton ion reacts with a negative chlorine ion in the presence of a third body. Most of the KrCl^* excimers are created either by three-body ion-ion recombination's (2.19, 2.20) or by harpooning

reactions (2.21). Three-body ion-ion recombination is a process in which two ions react in the presence of a third body. Harpooning reaction is a reaction in which an atom transfers their loosely bound electron to another atom/molecule and form ionic bond.



The reaction between Kr^* and Cl_2 does not always lead to the formation of KrCl^* . In that reaction, the excited Cl_2 molecule (Cl_2^*) can also be formed. The branching ratio for the formation of KrCl^* from such reactions is 0.9 and for Cl_2^* it is 0.1 [37,38]. By seeing the rate constants, one can conclude that the major mechanism for the formation of KrCl^* is the three body ion-ion recombination. In fact the contribution of the harpooning reaction process to the formation of KrCl^* is only about 5 to 6 percent [34]. The lifetime of KrCl^* is in the range of 5-9 ns [34]. Fig. 2.7 [39] shows the potential energy diagram of KrCl . As seen in Fig. 2.7 [39], the $B_{1/2} \rightarrow X_{1/2}$ transition of KrCl^* will emit UV radiation with an approximate energy of 6 eV. The reactions that lead to the formation of Cl_2^* and Cl_2^{**} are given below.



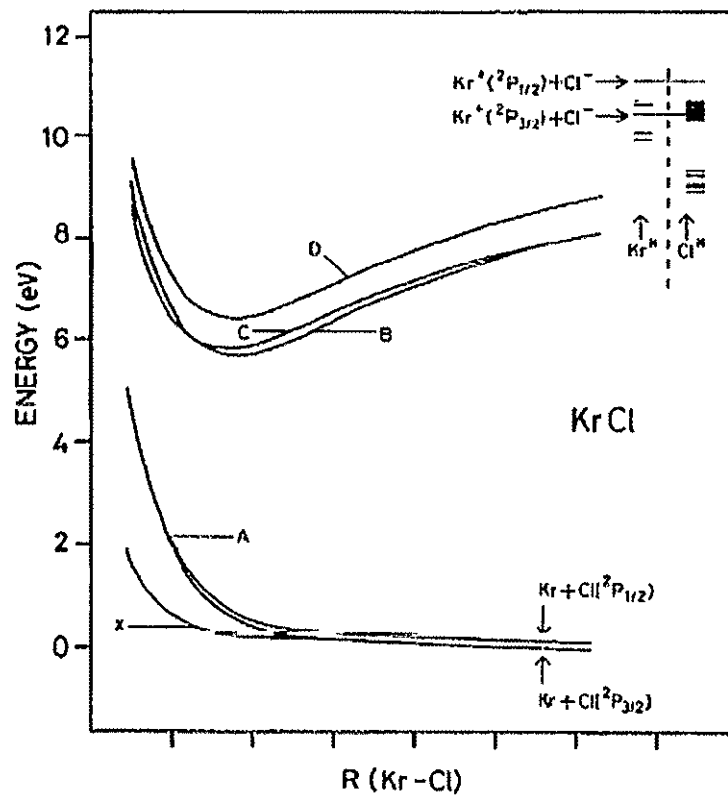
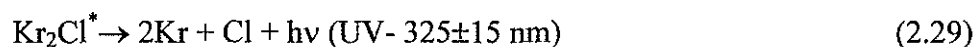
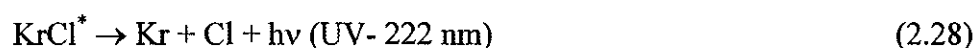


Fig. 2.7. Potential energy diagram of KrCl [39].

The average lifetime of Cl_2^* is 2.18 ns and that of Cl_2^{**} is 2.78 ns [40]. At high-pressures Kr_2Cl^* excimers can also be generated. These Kr_2Cl^* molecules are generated due to three body collisions between krypton atoms and the excited KrCl^* molecule.



Excimers formed are highly unstable and so quickly decompose giving up the extra energy present in them in the form of UV photons. So, when a discharge is generated in neon, krypton and chlorine gas mixture, the emission bands of KrCl^* , Kr_2Cl^* , Cl_2^* and Cl_2^{**} in the 200 to 350nm wavelength range are formed.



2.3 Applications of Excimer Lamps

Excimer UV and VUV radiation sources emit photons in the energy range of 3 to 10 eV. Such high-energy photons can dissociate several chemical bonds. So, excimer lamps can be used for a variety of photo-initiated volume and surface processes. The dissociation energies of several chemical bands and the wavelengths of different excimers are shown in Fig. 2.8 [41].

Recently, high intensity incoherent UV and VUV sources are being considered as an alternative to excimer lasers for industrial large scale low temperature materials processing [22]. This is because the excimer radiation emitted by these lamps is relatively cold, as the excimer lamps do not emit radiation in the infrared spectral range. Therefore heating of the irradiated material is largely avoided making them attractive for processing

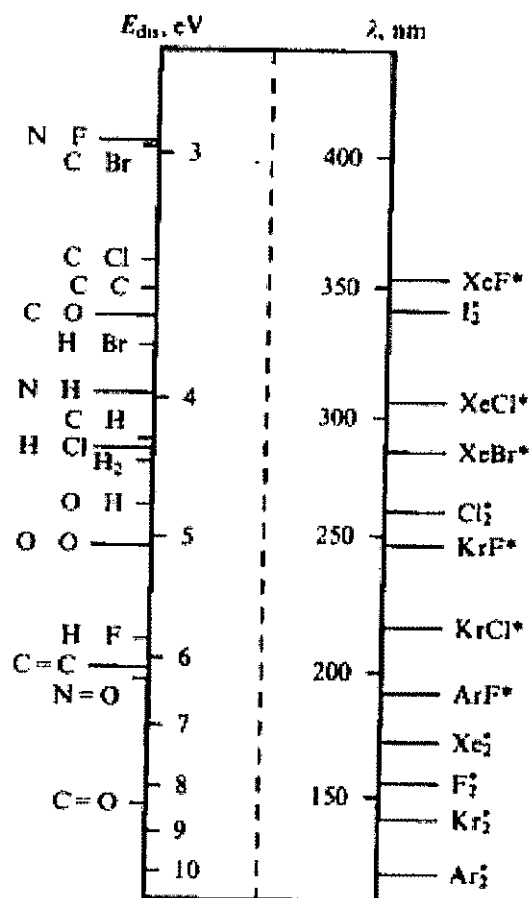


Fig. 2.8. Dissociation energies of several chemical bands and wavelengths of different excimer molecules [41].

heat-sensitive materials. A good quality silicon dioxide has been deposited using low temperature deposition technique [42]. The photo-induced thin film deposition of metals, semiconductors and dielectrics has become an important application of excimer lamps [11,33].

Excimer lamps are also used in the treatment of water. The use of excimer UV light for water treatment is considered, as other conventional methods used are not environmentally friendly [43,44]. Excimer lamps are best suited for this application because they do not use toxic materials like mercury, rendering them environmentally clean. This makes them a good alternative to replace chlorination for decontamination of drinking water.

One more area where excimer lamps are used is UV curing. UV curing is a process in which intense UV radiation is used to instantly cure paints, printing inks, varnishes, coatings and adhesives. UV curing is a high-speed photochemical process and operates at room temperature. Excimer lamps offer a number of advantages over other UV sources that make them attractive for UV curing. Excimer lamps emit radiation at very narrow wavelength range. So a perfect match to the absorption spectrum of the photo-initiator used in the process can be found. The photo-initiator molecules are responsible for the initiation of polymerization process. One more advantage of using excimer lamps for these purposes is that they do not use solvents and thereby eliminate the risk of emitting volatile organic compounds. Excimer lamps are also being used in the UV curing of optical fiber coatings [45]. In addition to the above-mentioned applications, these sources are required for many other applications, which include UV lithography, UV sterilization, air purification, photodecomposition and surface modification.

CHAPTER III

EXPERIMENTAL SET-UP AND PROCEDURES

3.1 Experimental Set-up

In our experiments, a cylindrical dielectric barrier discharge comprising a quartz tube with an outer ring electrode was used to generate UV radiation [23,24]. The experimental setup is shown in Fig. 3.1. The production of plasma requires a voltage of several kilovolts at frequencies in the kHz range to excite the gas in the discharge tube. So, a kHz amplifier along with a high voltage transformer that delivers an output voltage of up to 20 kilovolts is used. The kHz power amplifier amplifies the signal received from a signal generator and sends it to the high voltage (HV) transformer. The HV transformer further steps up the voltage and applies it across the electrodes of the device. The signal generator allows for control over the magnitude of the applied voltage and its frequency. A discharge is generated inside the tube when an AC voltage of several kilovolts, at a frequency of few kilohertz, is applied between the electrodes. The pressure in the quartz tube is monitored by a pressure gauge. The input voltage and the voltage across the series capacitor (introduced in the circuit in order to measure the charge Q accumulated by the electrodes) are measured with the help of an Oscilloscope (Tektronix, TDS 30328 model). High voltage probes (Tektronix, P6015A model) are used to measure voltages. A photograph of the actual system is shown in Fig. 3.2.

3.2 Electrode Configuration

The electrode geometry used in this system is very simple. A copper strap, which is wrapped outside the discharge tube and two stainless steel rings present at the ends of the discharge tube act as electrodes. The stainless steel ring electrodes are connected to

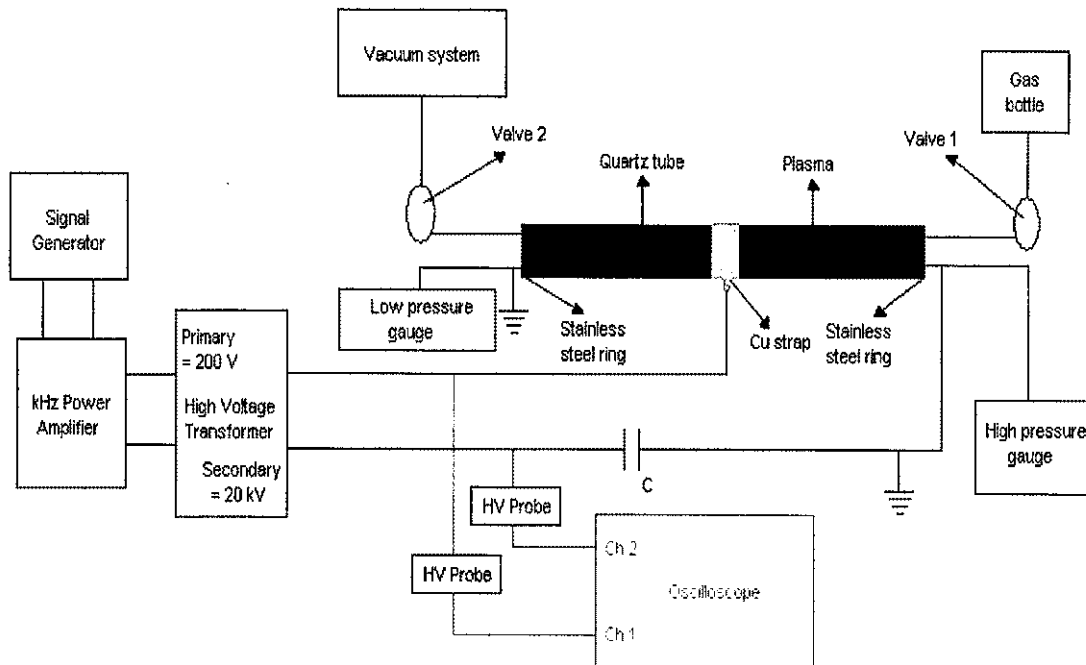


Fig. 3.1. Experimental set-up

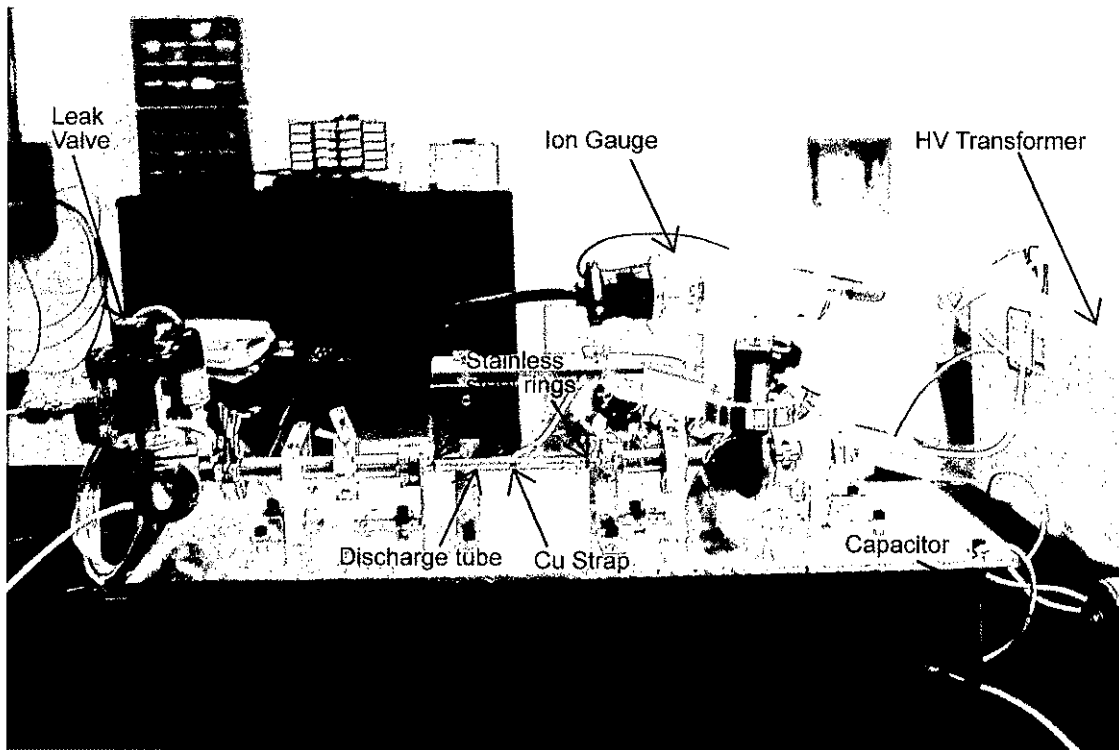


Fig. 3.2. Photograph of the actual system.

the ground. The discharge tube used is cylindrical in shape and is made up of quartz to allow the UV radiation to pass through (nearly 90% of radiation in 200 – 280 nm range can pass through [46]). Also quartz is a dielectric material and so the tube itself acts as a dielectric barrier, which is necessary in a dielectric barrier discharge system. Two 4.5-inch long quartz tubes of diameters 0.25 and 0.5 inch are used in our experiments. A simple sketch that depicts the electrode configuration is shown in Fig. 3.3. This type of arrangement of the electrodes has some advantages over the commercially available excimer lamps. In the commercial lamps, a wire mesh that acts as one of the electrode is present outside the tube all along its length. This results in less use of the generated radiation as the wire mesh partially blocks the UV light that is emitted by the lamp. One more disadvantage of the commercial lamp is the shortening of lifetime because of the presence of the internal electrode. If internal electrode comes in contact with the gas and contaminates the gas discharge, the lifetime of the lamp would be shortened. The system with the electrode geometry used in our experiments is advantageous because it neither uses the wire mesh all along the length of the discharge tube nor has any internal electrode. A photograph of the discharge tube is shown in Fig. 3.4.

3.3 Vacuum System

In our experiments, Alcatel vacuum pump and Leybold mechanical vacuum pump are used to evacuate the discharge tube. The Alcatel vacuum pump is used to evacuate the discharge tube before each experiment is started. Since the experiments must be run at relatively high pressures, as necessary for the formation of excimers, the Alcatel pump is switched off and the Leybold mechanical vacuum pump is used for maintaining the gas flow in the discharge tube.

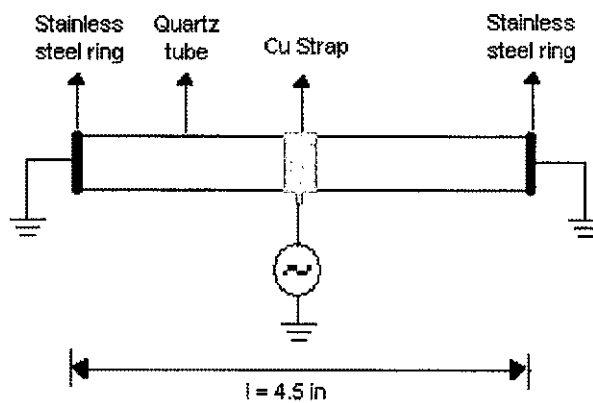


Fig. 3.3. Electrode configuration.

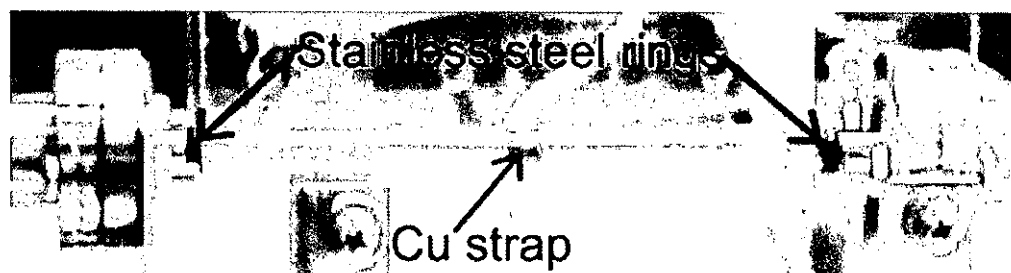


Fig. 3.4. Photograph of the discharge tube.

High pure environment is required for conducting the experiments. This is the reason for the use of the Alcatel vacuum pump as it has both mechanical and turbo pump, which can evacuate the chamber to a pressure of less than a millitorr range. Before each experiment is started, the discharge tube is evacuated to a pressure of 10^{-4} torr. Then the discharge tube is filled with pure gas mixture of neon, krypton and chlorine. To keep track of the pressure in the discharge tube, two pressure gauges are employed: a convection gauge and an ion gauge. The convection gauge measures the pressure in 1millitorr to atmospheric pressure range. To measure the pressure below 1 millitorr, an ion gauge is used.

3.4 Spectroscopy Set-up

Spectral measurements were performed using a 0.5-meter triple grating 0.5 m monochromator/spectrograph, SpectroPro 500i model. A photo multiplier tube added to the internal spectrometer setup is shown in Fig. 3.5 [47]. The light that enters from the entrance slit passes through a combination of mirrors, gratings and comes out through the exit slit as monochromatic light. The wavelength of the light coming out can be controlled. This light (photons) then enters a photo multiplier tube (PMT). In all our spectral measurements, a voltage of 900 volts is applied to the PMT. This tube converts photons flux into electrical current. The amount of current generated is determined by the rate of photons entering the tube. So by using a spectrometer, the relative intensity of the light at each wavelength can be known.

The SpectroPro 500i can be operated by using a computer through RS232 interface or by using a remote scan controller. In our experiments, we used a computer to operate the monochromator. The entrance and exit slits are adjustable in the range of 10

to 3000 micrometers. In our spectral measurements, a slit width of 200 micrometer for both the entrance and exit slits is used. For better resolutions, grating of 1200 g/mm and wavelength step of 0.2 nm are used. Each scan is done in the wavelength range of 180-350 nm, always starting from lower wavelength value. As the UV radiation in the range of interest (200 – 300 nm) can travel in air for a short distance, no vacuum is necessary between the discharge tube and entrance slit of the spectrometer. However the spectrometer is placed close to the discharge tube as the intensity of UV radiation decreases rapidly as it travels in air.

3.5 Measurements

3.5.1 Power calculations

The electrical power consumed by the plasma is calculated from the Q-V graph using the Lissajous method [21]. To measure the charge a capacitor was inserted in the circuit. The capacitor used should have a higher capacitance value than that of the plasma device equivalent capacitance in order to have most of the voltage drop across the plasma capacitance (C_p). In this experiment capacitor having a capacitance (C) of 2nF is used. The equivalent electrical circuit of the discharge is shown in Fig. 3.6. The input voltage (V) and the voltage across the capacitor (V_C) are measured with the help of an oscilloscope. Then charge (Q) in the circuit can be calculated using:

$$Q = C * V_C \quad (3.1)$$

The electrical power consumed by the discharge is the product of applied voltage and current in the circuit. Electrical power consumed is also equal to the product between area enclosed in the Q-V graph of the circuit and applied frequency:

$$\text{Power consumed} = V * I = V * (Q * F) = (Q * V) * F \quad (3.2)$$

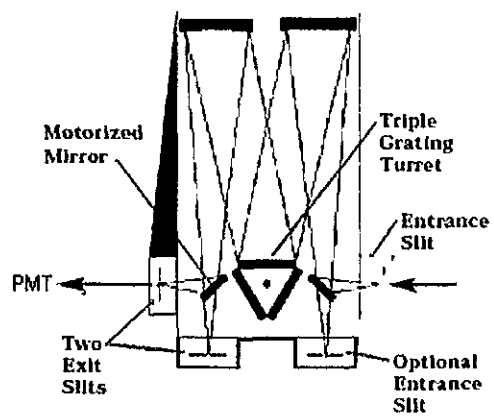


Fig. 3.5. Internal spectrometer setup [47].

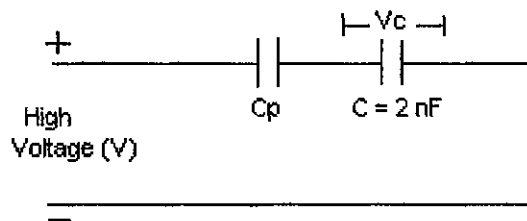


Fig.3.6. Equivalent electrical circuit of the discharge.

$$\Rightarrow \text{Power consumed} = \text{Area enclosed in the Q-V graph} * \text{Frequency} \quad (3.3)$$

where V is the applied voltage, V_C is the voltage across the capacitor and F is the applied frequency. The area enclosed in the Q-V graph is calculated using Matlab. The frequency of the applied input voltage can be obtained from the oscilloscope.

3.5.2 Efficiency calculations

If the power consumed by the lamp and the UV radiation emitted by the lamp is known, then the efficiency can be calculated using:

$$\text{Efficiency} = \text{UV power emitted by lamp} / \text{Power consumed by the lamp} \quad (3.4)$$

The power consumed by the lamp is calculated using the lissajous method described above in the power calculations section [3.5.1]. The total UV power emitted is the amount of radiation power present over an integrated area around the discharge tube. To find out the total UV power emitted by the lamp, the power density of the UV radiation emitted must be known. After measuring the power density with a calibrated UV photometer (International Light, SEL 220 model), the UV power emitted by the lamp can be calculated using:

$$\text{UV power emitted} = 2 * \Pi * h * l * \text{Power density} \quad (3.5)$$

where l is the length of the discharge tube, h is the distance between the lamp and the photometer, which is used to measure the UV power density. Experimental setup for measuring the UV power density is shown in Fig. 3.7.

The photometer used is calibrated to measure the power density of the UV radiation in wavelength range of 200-300 nm. The calibrated UV photometer measures the power density in units of mW/cm^2 . All the UV power density measurements are taken at a distance of 2 inch (5.08 cm) away from the discharge tube.

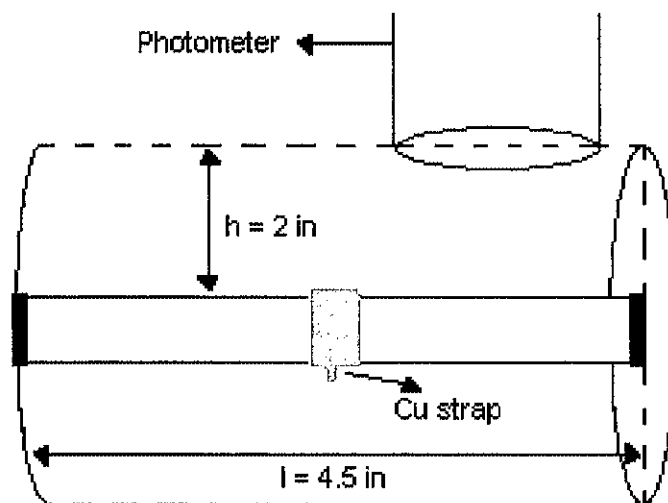


Fig. 3.7. Experimental setup for measuring UV power density.

CHAPTER IV

RESULTS AND DISCUSSION

The emission spectrum of the discharge in neon, krypton and chlorine gas mixture for different combinations of pressure (p) in the discharge, voltage (V) and frequency (f) of the input signal and diameter (d) of the discharge tube is observed. In all these experiments, our main aim is on how to increase the intensity of UV radiation in the wavelength range of 200 to 280 nm. To achieve this objective, the dependence of the intensity of UV radiation on different operating parameters (pressure, voltage and frequency of the input signal and discharge tube diameter) is studied and analyzed using a spectrometer and UV calibrated photometer. The spectrometer gives the relative intensity of the radiation at different wavelengths. By using the spectrometer, the UV radiation intensities at the KrCl^* and Cl_2^* emission bands are noted. These values are used to evaluate the dependence of the UV radiation intensity on the four operating parameters. The UV calibrated photometer gives the actual power density of the UV radiation integrated over a specific spectral range. A photometer which measures the power density in units of mW/cm^2 in the 200 to 300 nm spectral range, where the emission bands of Cl_2^{**} , KrCl^* and Cl_2^* are present, is used in our experiments. The effect of operating parameters on the electrical power consumed by the lamp to generate UV radiation is studied. The effect of pressure and electrical power consumed on the efficiency of the lamp are also observed. The results obtained are presented in this chapter.

4.1 Power Measurements

A research grade gas mixture of Neon (89.9%), Krypton (10%) and Chlorine (0.1%) gases in the ratio given in the brackets is used in our experiments to generate UV

radiation. The electrical power consumed by the lamp is calculated from the Q-V graph using the Lissajous method. The procedure used to calculate the power consumed is discussed in chapter 3. Fig. 4.1 shows how charge and voltage vary with respect to time. Fig. 4.2 shows the Q-V graph (Lissajous figure) of the discharge in Ne/Kr/ Cl₂ gas mixture at a voltage of 8 kV, frequency of 18 kHz, pressure of 150 torr and discharge tube diameter of 0.25 inch. The area enclosed by this Q-V graph is calculated using matlab. The power consumed can be obtained by multiplying the frequency of the input signal with the area enclosed by the Q-V graph. The power consumed to generate UV radiation is calculated for various combinations of operating parameters. The effect of these parameters on the electrical power consumed by the lamp is studied.

Our first observation is that the electrical power consumed by the lamp doesn't change much with pressure. However, as seen in Fig. 4.3, the electrical power consumed by the lamp is an increasing function of the input voltage. Fig. 4.4 shows the power consumed by the lamp as a function of Frequency. The electrical power consumed by the lamp varies with the frequency of the input signal. An increase in the frequency of the input signal results in an increase of the electrical power consumed by the lamp. Fig. 4.5 shows the electrical power consumed by the lamp for different discharge tube diameters as a function of pressure. For a particular discharge tube diameter, it can be seen that there is no change in the power consumed with pressure. However an increase in the diameter of the discharge tube leads to an increase in the electrical power consumed by the lamp.

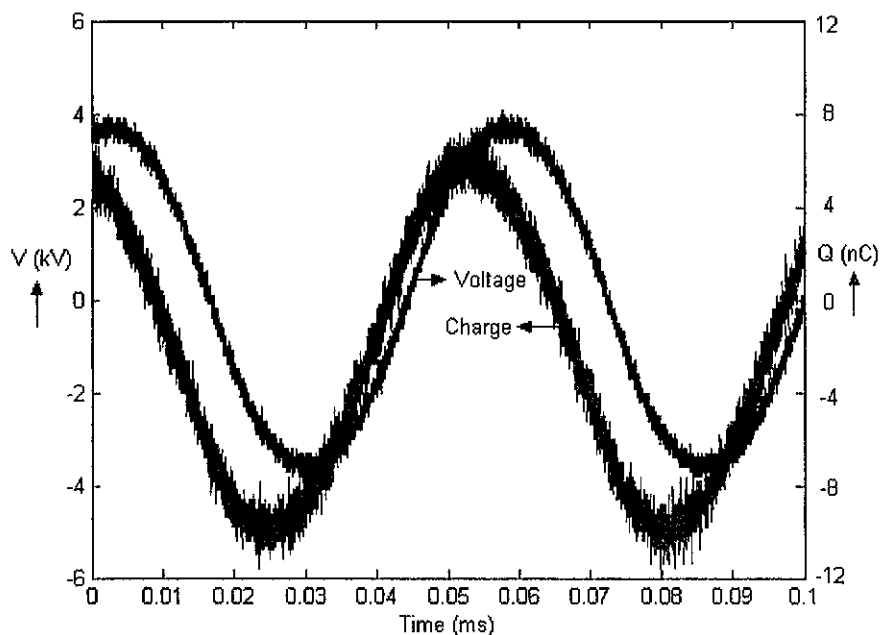


Fig. 4.1. Charge and Voltage vs. Time: Discharge in Ne/Kr/ Cl₂ gas mixture at $V = 8$ kV, $f = 18$ kHz, $p = 150$ torr. The diameter of the discharge tube is 0.25 in.

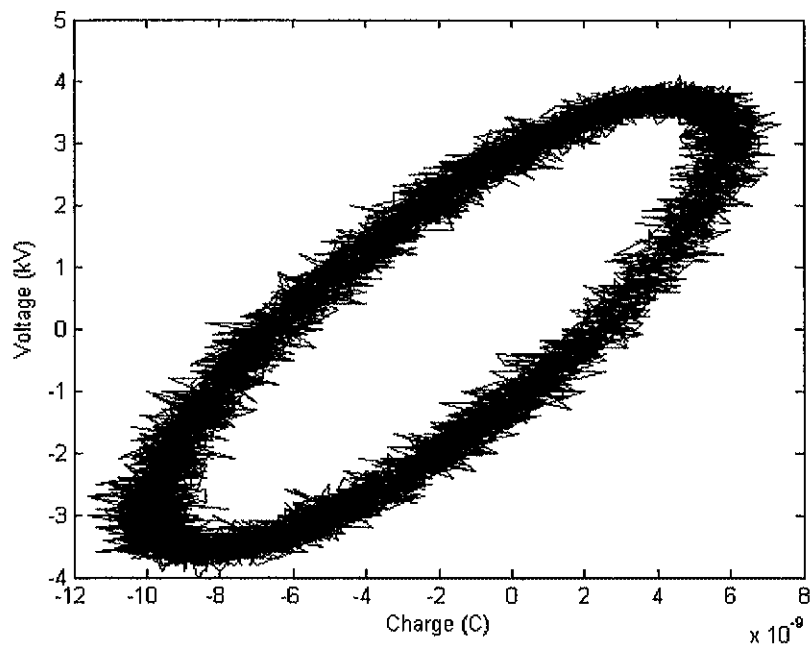


Fig. 4.2. Q-V graph (Lissajous figure) of the Discharge at $V = 8$ kV, $f = 18$ kHz, $p = 150$ torr. The diameter of the discharge tube is 0.25 in.

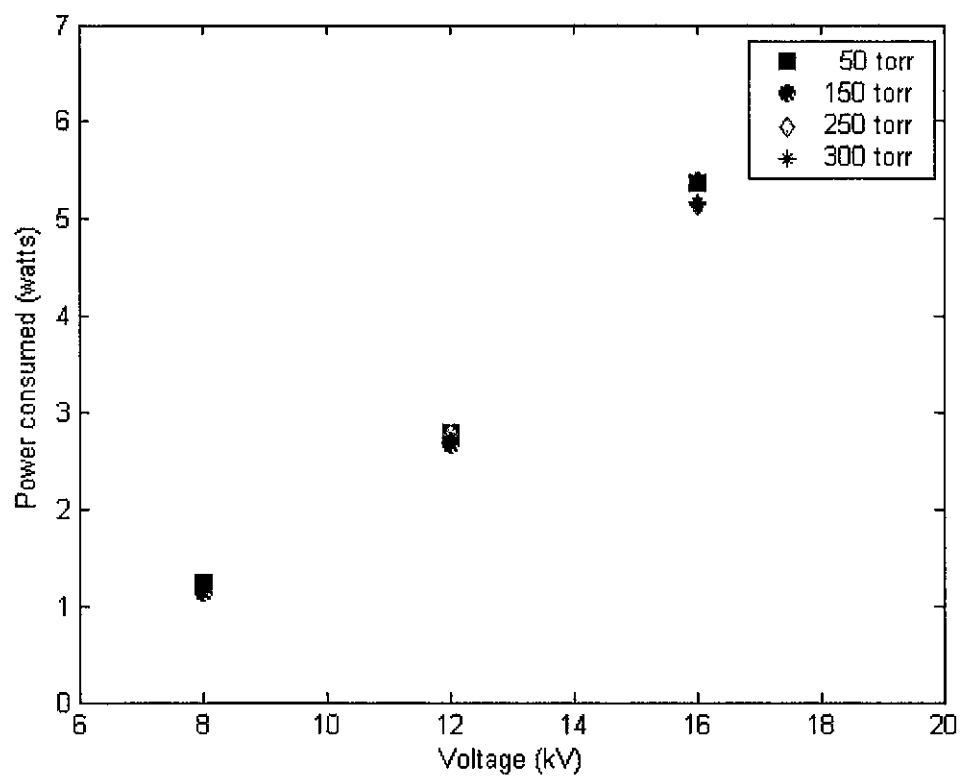


Fig. 4.3. Power consumed by the lamp as a function of Voltage for different pressures at a frequency of 18 kHz. The diameter of the discharge tube is 0.25 in.

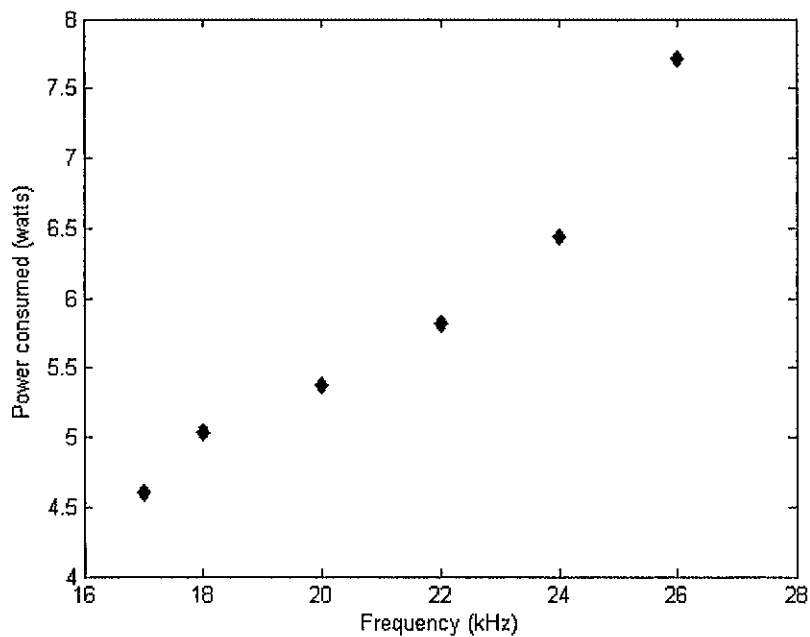


Fig. 4.4. Power consumed by the lamp as a function of Frequency at a voltage of 14 kV and pressure of 100 torr. The diameter of the discharge tube is 0.25 in.

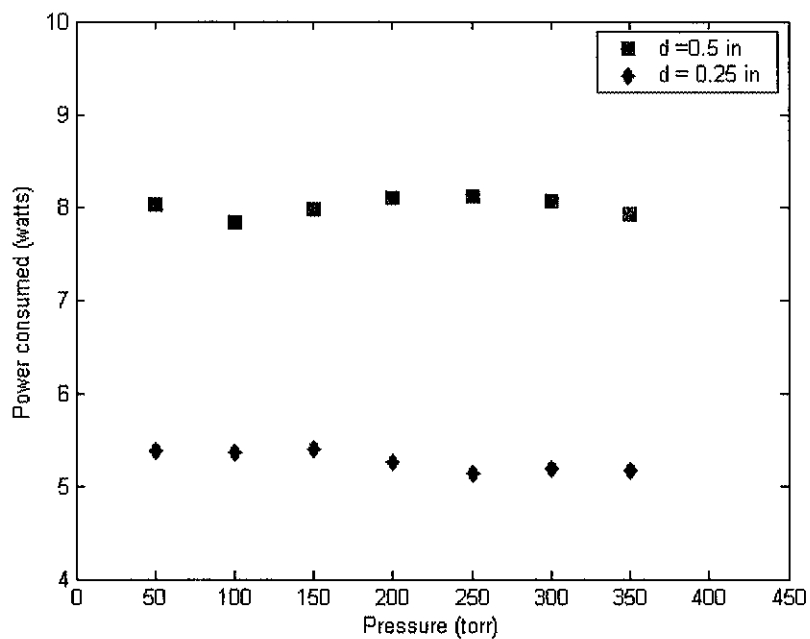


Fig. 4.5. Power consumed by the lamp as a function of Pressure for different discharge tube diameters at a frequency of 18 kHz and voltage of 16 kV.

4.2 Emission Spectroscopy

The emission spectrum of the discharge in the neon, krypton and chlorine gas mixture in the UV range of 180 - 350 nm is shown in Fig. 4.6. The emission spectrum obtained is similar to the one reported by Shuaibov et al [48]. Strong emission bands are observed at 200 nm (Cl_2^{**}), 222 nm (KrCl^*) and 258 nm (Cl_2^*). The Kr_2Cl^* emission band is also observed in the spectrum. As seen in Fig. 4.6, the Kr_2Cl^* excimers emit UV radiation in a broad wavelength range (325 ± 15 nm). The emission spectrum of the discharge in Ne/Kr/ Cl_2 gas mixture is mainly dominated by the Cl_2^* emission band. This is because of the presence of buffer gas (Ne) in the gas mixture. Boyd et al [12], found out that when a buffer gas is present in the gas mixture, the emission spectrum showed an increase at the 258 nm emission peak. Also the intensity of KrCl^* emission band without buffer gas will always be higher than that generated using the buffer gas in the gas mixture at the same pressure [12]. This is because the buffer gas (Ne) present in the gas mixture will often displace the Kr atom in many collision processes, which lead to the formation of KrCl^* . The full width half maximum (FWHM) for the KrCl^* and Cl_2^* emission bands varied with pressure. The FWHM for KrCl^* emission band is between 2 to 4 nm. The FWHM for Cl_2^* emission band is between 9 to 11 nm. A photograph of the discharge at a voltage of 16 kV is shown in Fig. 4.7. The discharge appears reddish in color near the copper strap and bluish elsewhere.

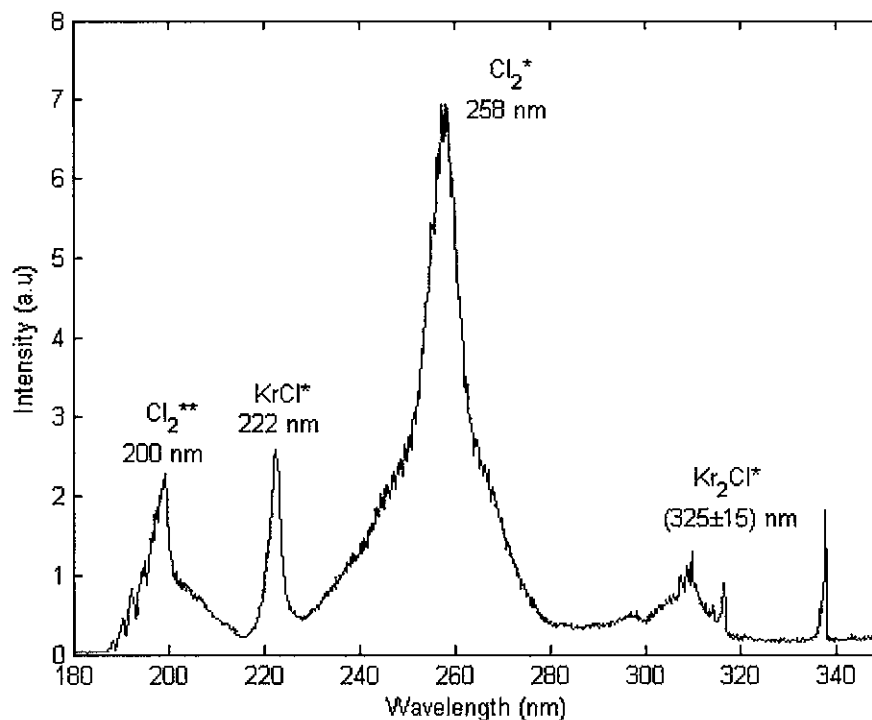


Fig. 4.6. Emission spectrum of the Discharge in Ne/Kr/ Cl_2 gas mixture at $V = 16$ kV, $f = 18$ kHz, $p = 250$ torr. The diameter of the discharge tube is 0.25 inch.

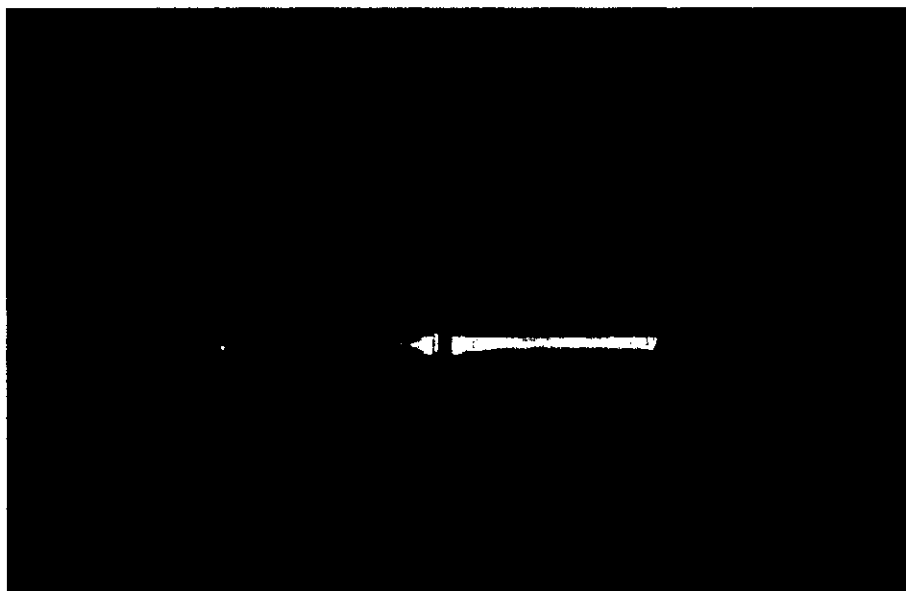


Fig. 4.7. Picture of the Discharge at $V = 16$ kV, $f = 18$ kHz, $p = 250$ torr. The diameter of the discharge tube is 0.25 inch.

4.3 Spectral Measurements

Emission spectra for different combinations of the operating parameters are observed and the dependence of the intensity of UV radiation from KrCl^* and Cl_2^* emission bands on them is studied. While studying the effect of one parameter on the UV radiation intensity, the other three are kept constant at a particular value.

4.3.1 Effect of Pressure

Fig. 4.8 shows the effect of pressure on the intensity of KrCl^* and Cl_2^* emission bands. It can be seen that both the emission bands at 222 nm and 258 nm showed the same behavior with the change in pressure. The intensity of the emission bands increased with increase in the pressure until it reaches a maximum value; after that the intensity decreased with pressure. The maximum intensity for both the emission bands is achieved at a pressure of 250 torr. Since the electrical power consumed by the discharge does not vary much with pressure, the decrease in the intensity of emission bands after 250 torr is mainly caused due to the formation of more triatomic excimers (Kr_2Cl^*). Kr_2Cl^* are formed as a result of the three body collisions of KrCl^* and rare gas atoms. It can be seen from the Fig. 4.9, that the intensity of Kr_2Cl^* emission band is increasing and that of KrCl^* emission band is decreasing as the pressure is increased over 250 torr. The emission spectra of the discharge operated at 250 torr and 450 torr are shown in Fig. 4.10. The formation of triatomic excimers is favored at high pressures. The intensity of Kr_2Cl^* emission band is increasing with the pressure in the discharge. At a pressure of 450 torr, the intensity of Kr_2Cl^* emission band is even greater than that of KrCl^* emission band (Fig. 4.10).

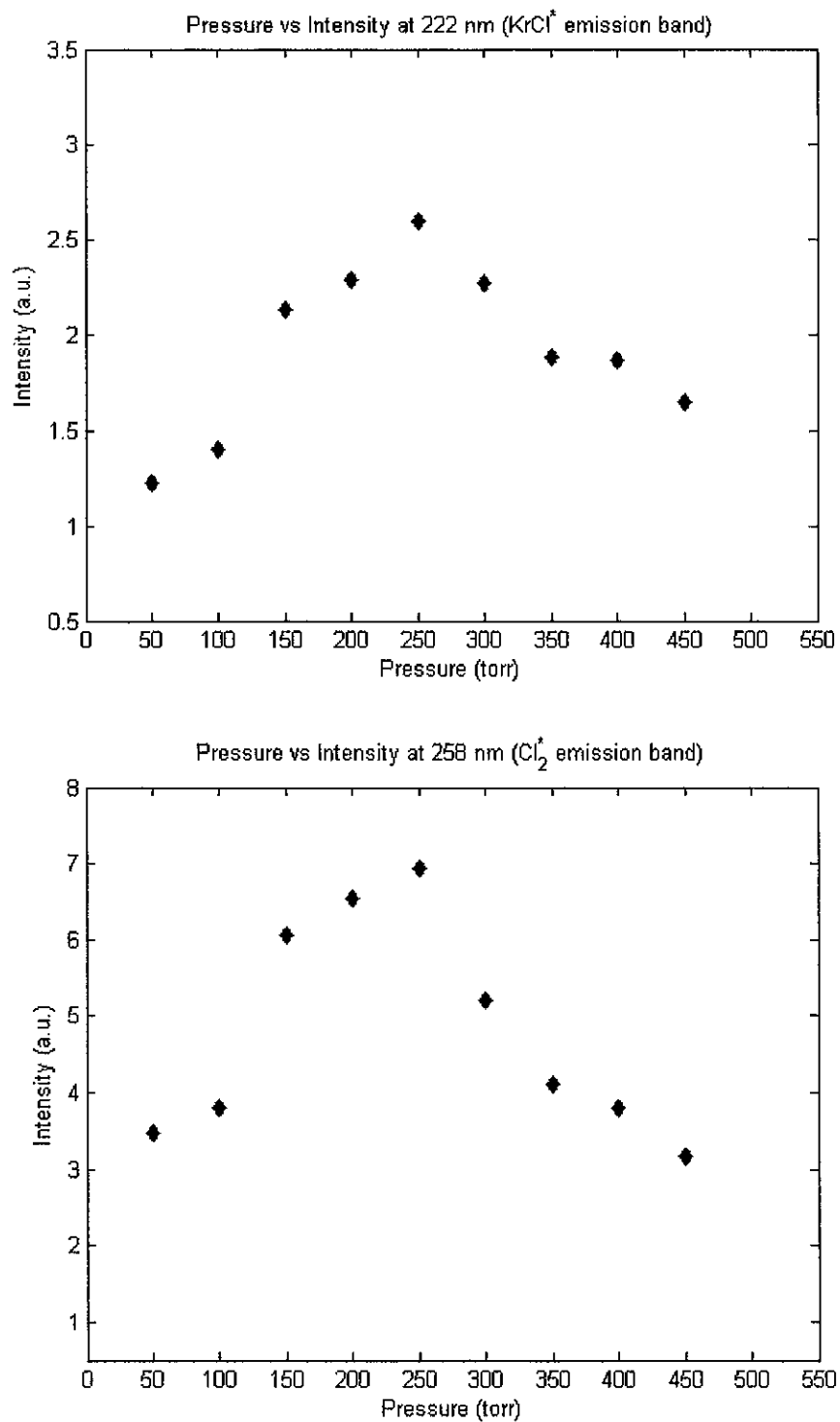


Fig. 4.8. Intensity of KrCl⁺ and Cl₂⁺ emission bands as a function of Pressure at V = 16 kV, f = 18 kHz. The diameter of the discharge tube is 0.25 inch.

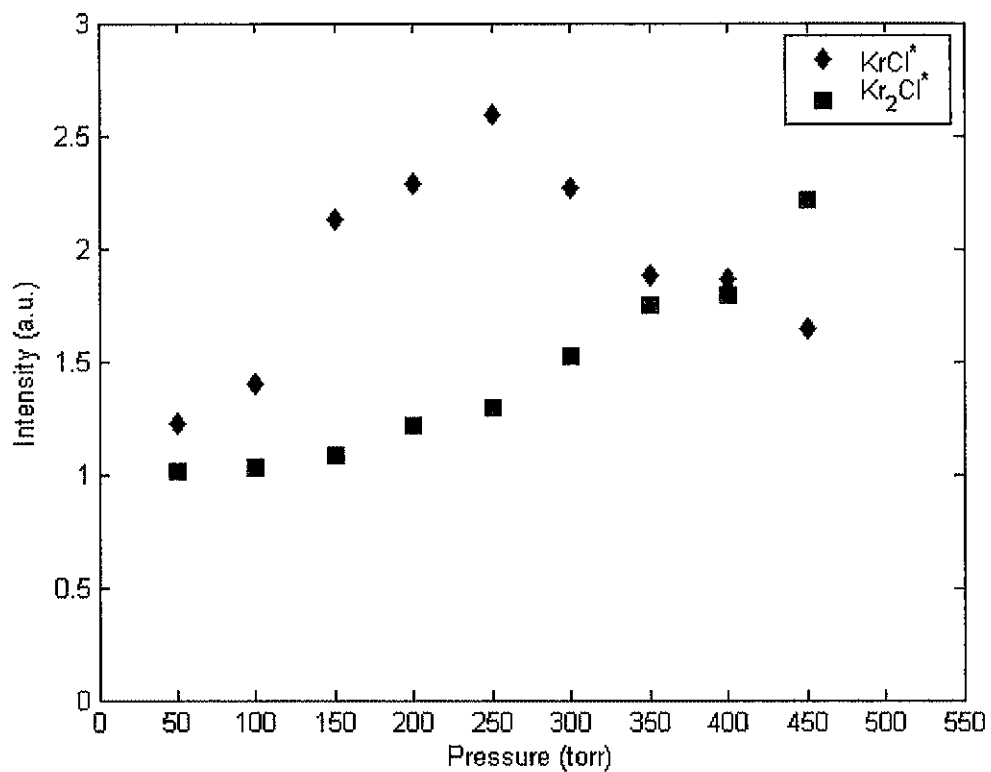


Fig. 4.9. Intensity of KrCl^* and Kr_2Cl^* emission bands as a function of Pressure at $V = 16$ kV, $f = 18$ kHz. The diameter of the discharge tube is 0.25 inch.

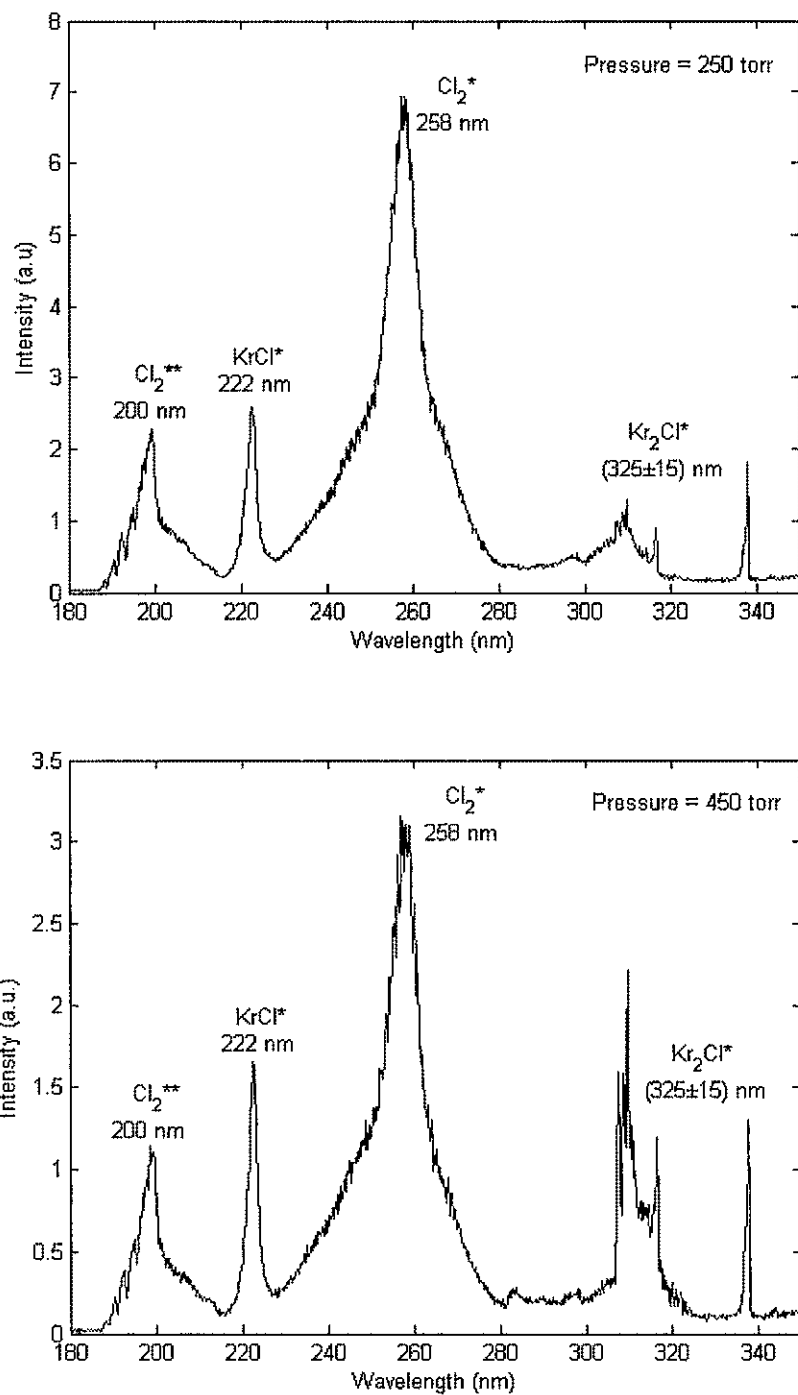


Fig. 4.10. Emission spectrum of the Discharge in Ne/Kr/Cl₂ gas mixture at pressures of 250 and 450 torr: V = 16 kV, f = 18 kHz. The diameter of the discharge tube is 0.25 inch.

4.3.2 Effect of Voltage

The effect of voltage on the intensity of KrCl^* and Cl_2^* emission bands is shown in Fig. 4.11. It can be observed that both the emission bands centered around 222 nm and 258 nm show the same behavior with a change in voltage. The intensity of the KrCl^* and Cl_2^* emission bands are found to be increasing as the voltage is increased. The increase in the intensity of the emission bands is due to increase in the power consumed by the discharge, which leads to a higher production of excimers. The change in the power consumed by the discharge with respect to voltage is shown in the Fig. 4.3.

4.3.3 Effect of Frequency

The effect of frequency on the intensity of KrCl^* and Cl_2^* emission bands is shown in Fig. 4.12. It can be seen that both the emission bands around 222 nm and 258 nm show the same behavior with the change in frequency. The maximum intensity is achieved at 18 kHz. With increase in the frequency over 18 kHz, the intensity of the KrCl^* and Cl_2^* emission bands is found to be decreasing. Since the power consumed by the discharge increases with frequency, this decrease in intensity of the KrCl^* and Cl_2^* emission bands beyond the frequency of 18 kHz is attributed to the formation of more Kr_2Cl^* excimers. At frequencies greater than 18 kHz, more triatomic excimers (Kr_2Cl^*) are formed as a result of the three body collisions of KrCl^* and the krypton atoms. The emission spectra of the discharge operated at frequencies of 3, 18, 23 and 25 kHz is shown in Fig. 4.13. The intensity of Kr_2Cl^* emission band is increasing and that of KrCl^* and Cl_2^* emission bands is decreasing as the frequency is increased over 18 kHz.

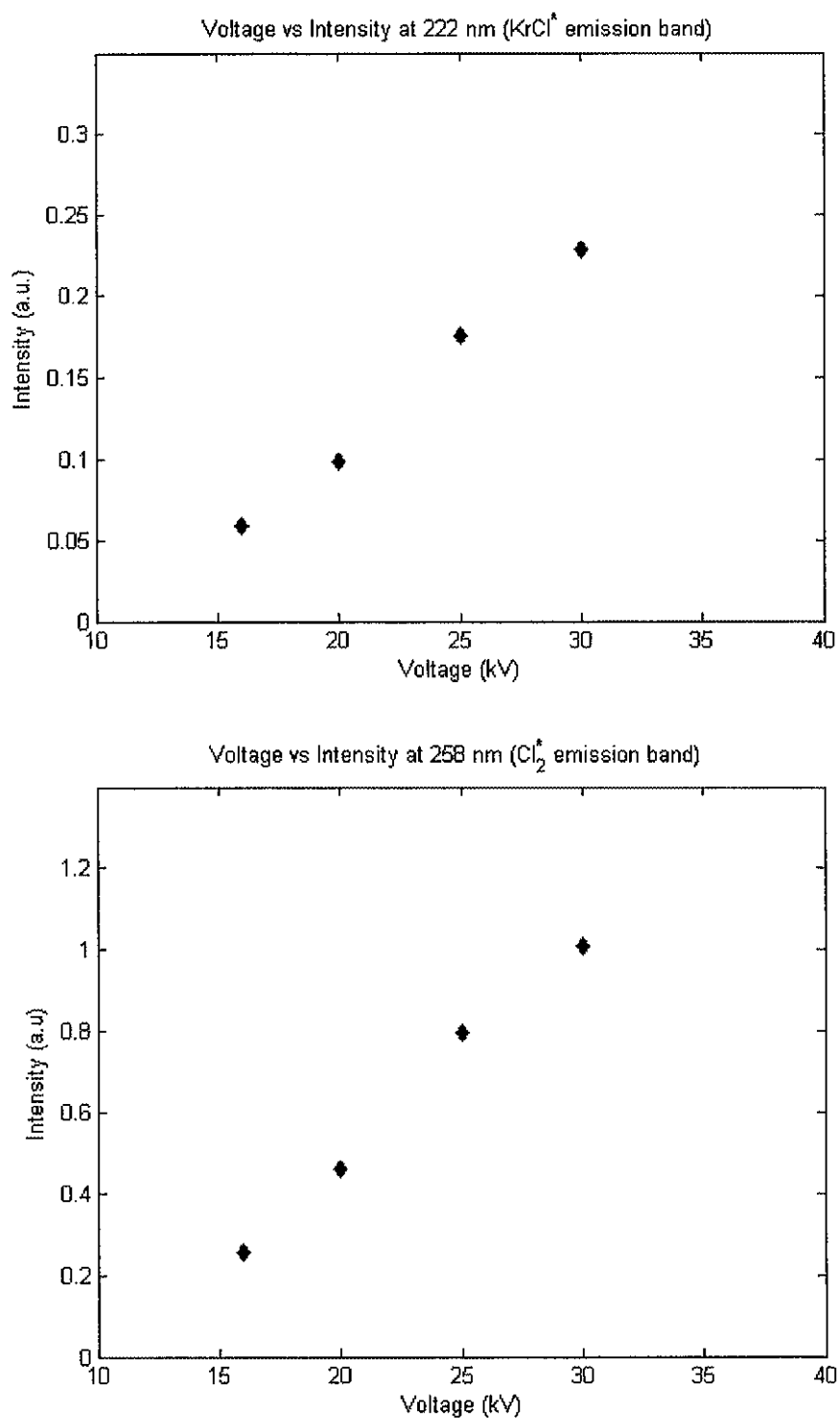


Fig. 4.11. Intensity of KrCl^* and Cl_2^* emission bands as a function of Voltage at $p = 25$ torr, $f = 3$ kHz. The diameter of the discharge tube is 0.25 inch.

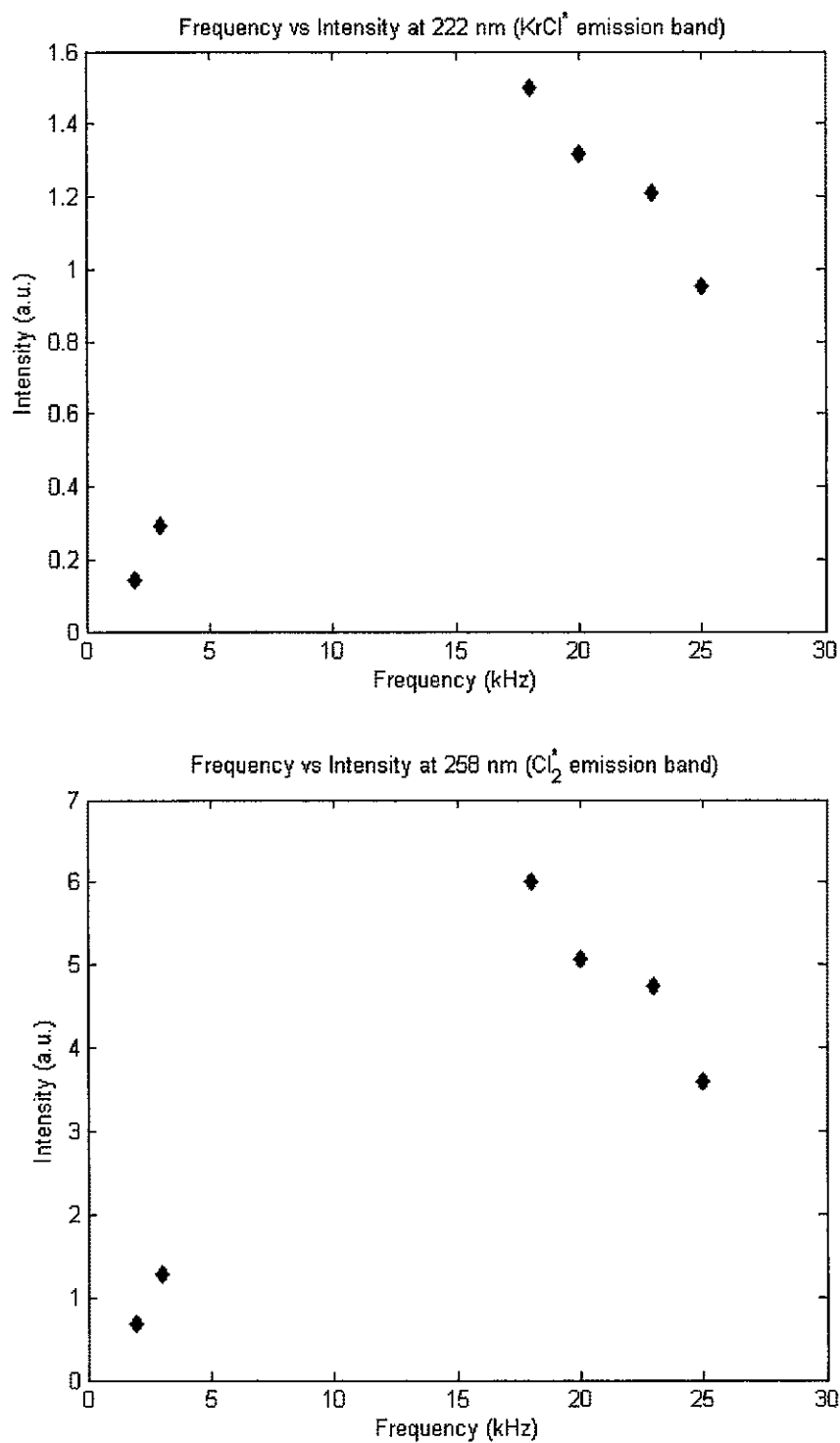


Fig. 4.12. Intensity of KrCl* and Cl₂* emission bands as a function of Frequency at p = 25 torr, V = 16 kV. The diameter of the discharge tube is 0.25 inch.

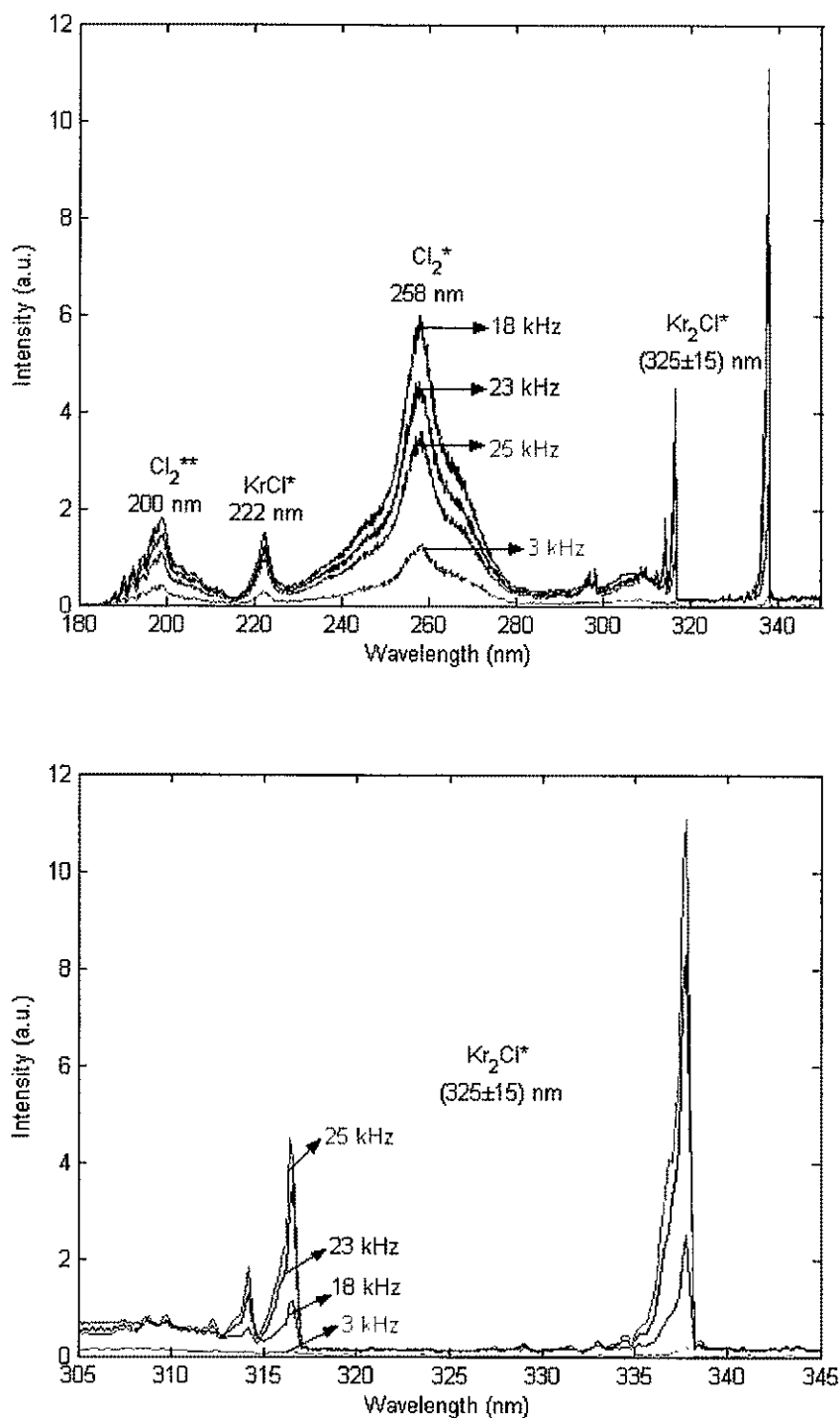


Fig. 4.13. Emission spectrum of the Discharge in Ne/Kr/Cl₂ gas mixture at frequencies of 3, 18, 23 and 25 kHz: V = 16 kV, p = 25 torr. The diameter of the discharge tube is 0.25 inch.

4.3.4 Effect of Discharge tube diameter

The effect of the diameter of the discharge tube on the intensity of KrCl^* and Cl_2^* emission bands is shown in Fig. 4.14. It can be seen that there is an increase in the intensity of UV radiation with increase in the diameter of the tube. The increase in the intensity of the emission bands is simply due to a larger plasma volume, which leads to a higher number of excimers generated, but which requires an increase in the power consumed by the discharge. The power consumed by the discharge at different pressures for both the discharge tubes is shown in the Fig. 4.5.

4.4 Power Density Measurements

The dependence of intensity on a) frequency; b) voltage; c) pressure; and d) discharge tube diameter is also analyzed by the determination of the UV power density values emitted by the discharge, which are measured using photometer. In this section, the dependence of the UV radiation intensity on the discharge operating parameters is analyzed using the absolute power density emitted by the discharge in the 200-300 nm wavelength range. A calibrated photometer (International light, SEL 220 model) that gives the power density of the UV radiation in milliwatts per square centimeter (mW/cm^2) in a specific wavelength range of 200-300 nm, where the emission bands of Cl_2^{**} , KrCl^* and Cl_2^* are present, is used in our measurements. Since the emission of Kr_2Cl^* excimers is in the spectral range of 325 ± 15 nm, the photometer does not measure the intensity of the Kr_2Cl^* emission band.

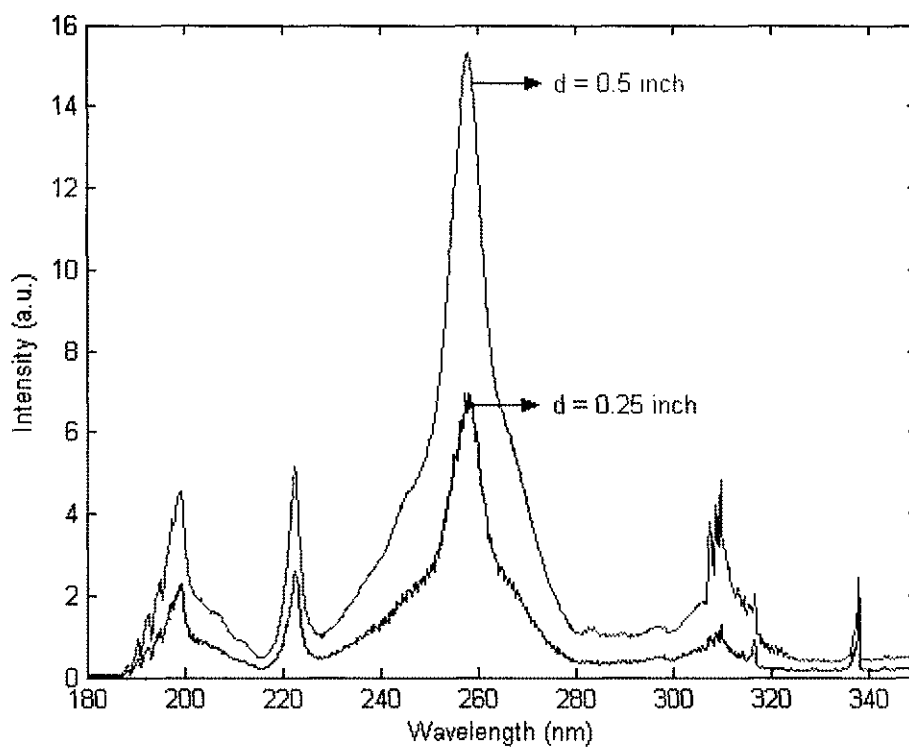


Fig. 4.14. Emission spectrum of the Discharge in Ne/Kr/Cl₂ gas mixture for two different discharge tubes of diameter 0.25 and 0.5 inch at $V = 16$ kV, $p = 250$ torr and $f = 18$ kHz.

4.4.1 Effect of Pressure

The effect of pressure on the UV power density of the radiation is shown in Fig. 4.15. The power density of the discharge radiation increased with increase in the pressure until it reached a maximum value after which the power density decreased with pressure. The maximum power density is achieved at a pressure of 250 torr. As the power consumed does not vary much with pressure, the decrease in the power density of the discharge after 250 torr must be mainly caused due to the formation of more Kr_2Cl^* excimers. Kr_2Cl^* are formed as a result of the three body collisions of KrCl^* and krypton atoms. This is well correlated by Fig. 4.9, which shows that the intensity of KrCl^* emission band decreases while that of Kr_2Cl^* emission band increases as the pressure is increased over 250 torr. Though the Kr_2Cl^* emission band (325 ± 15 nm) intensity is increasing, the photometer measures a decrease in the UV radiation intensity after 250 torr because the emission of Kr_2Cl^* falls outside the range of 200-300 nm. The UV power density emitted by the discharge, as measured by the photometer (see Fig. 4.15), shows the same pressure dependence as that of the intensity of KrCl^* and Cl_2^* emission bands recorded by the spectrometer (see Fig. 4.8).

4.4.2 Effect of Voltage

The effect of voltage on the UV power density of the radiation is shown in Fig. 4.16. The power density of the UV radiation is found to be an increasing function of the voltage. The increase in the UV power density is due to the increase in the power consumed by the discharge with the voltage. The change in the electrical power consumed by the discharge with respect to voltage was shown earlier in Fig. 4.3. The UV

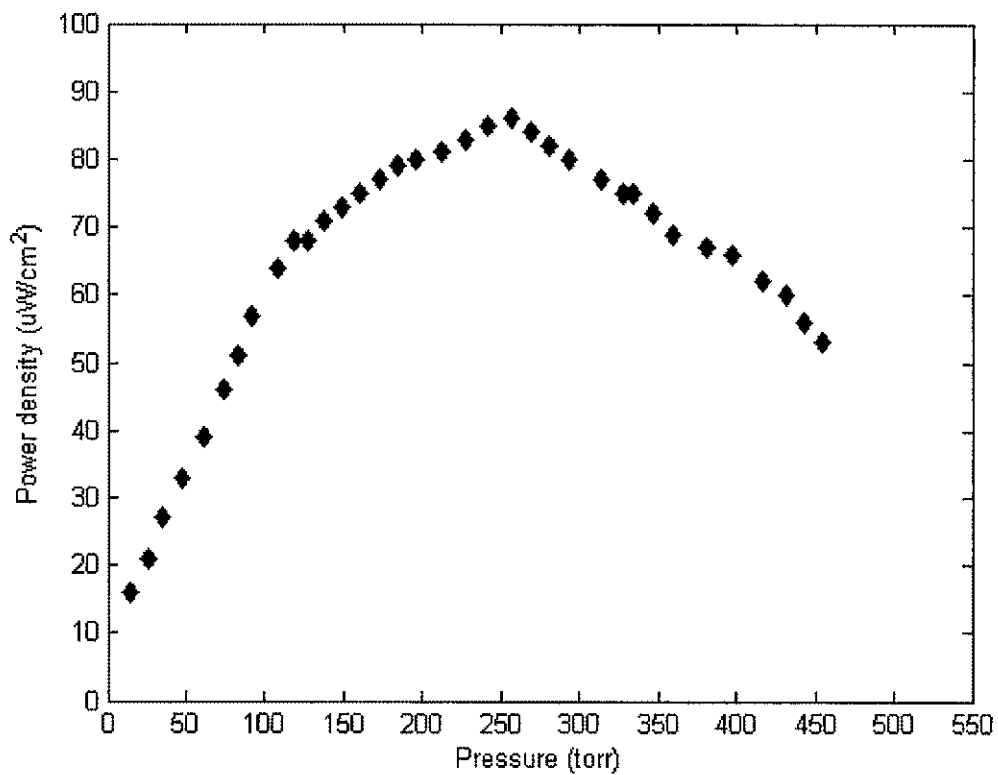


Fig. 4.15. Power density of the discharge as a function of Pressure at $V = 16$ kV, $f = 18$ kHz. The diameter of the discharge tube is 0.25 inch. UV photometer is placed 2-inch from source.

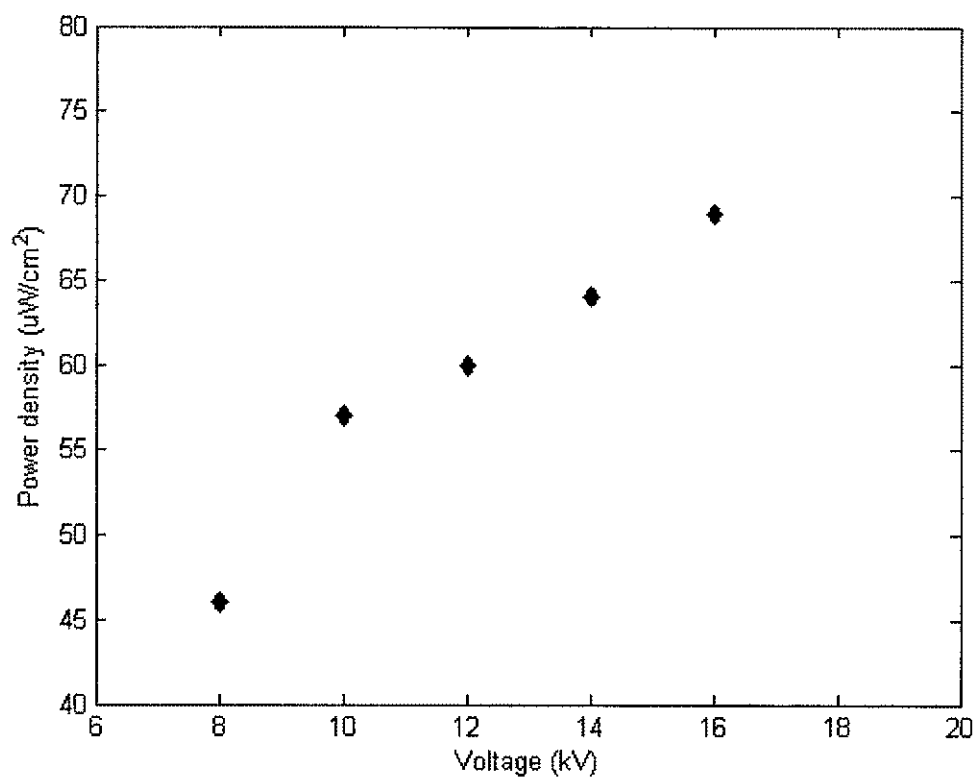


Fig. 4.16. Power density of the discharge as a function of Voltage at $f = 18$ kHz, $p = 100$ torr. The diameter of the discharge tube is 0.25 inch. UV photometer is placed 2-inch from source.

power density emitted by the discharge (see Fig. 4.16) showed the same voltage dependence as that of the intensity of KrCl^* and Cl_2^* emission bands (see Fig. 4.11).

4.4.3 Effect of Frequency

The effect of frequency on the power density of UV radiation emitted as a result of discharge in Ne/Kr/ Cl_2 gas mixture is shown in Fig. 4.17. The UV power density emitted by the discharge and measured by the photometer (Fig. 4.17) showed the same frequency dependence as that of the intensity of the KrCl^* and Cl_2^* emission bands measured by the spectrometer (Fig. 4.12). Here also the maximum intensity is achieved at 18 kHz. With increase in the frequency over 18 kHz, the intensity of the UV radiation is found to be decreasing. As power consumed by the plasma is not decreasing with increase in frequency (Fig. 4.4), the reason for the decrease in intensities over 18 kHz is mainly due to the formation of more triatomic excimers (Kr_2Cl^*).

4.4.4 Effect of Discharge tube diameter

The effect of the diameter of the discharge tube on UV power density is shown in Fig. 4.18. It can be seen that there is an increase in the power density of UV radiation with increase in the diameter of the tube. The increase in the UV power density is due to increase in the power consumed by the discharge when a large diameter tube is used. The power consumed by the discharge at different pressures for both the discharge tubes was shown earlier in Fig. 4.5.

4.5 Efficiency Measurements

The conversion efficiency (output UV power/ electrical power consumed) of the lamp is obtained by using the data from the calibrated photometer and the Lissajous technique. The efficiency versus pressure for both discharge tube diameters is shown in

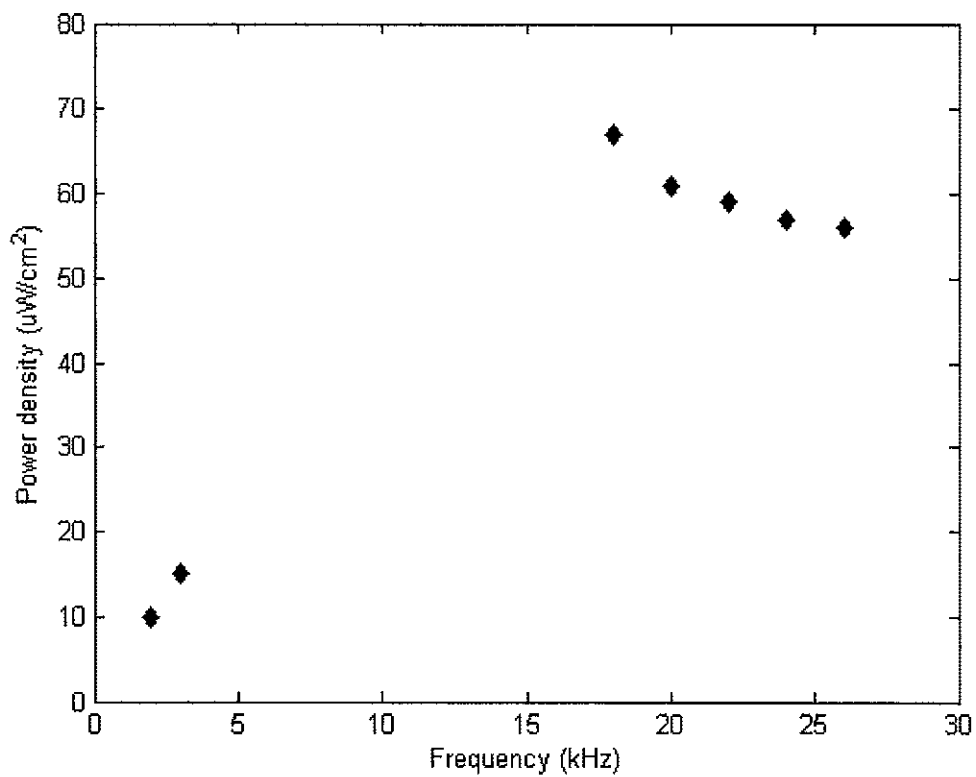


Fig. 4.17. Power density of the discharge as a function of Frequency at $V = 16$ kV, $p = 100$ torr. The diameter of the discharge tube is 0.25 inch. UV photometer is placed 2-inch from source.

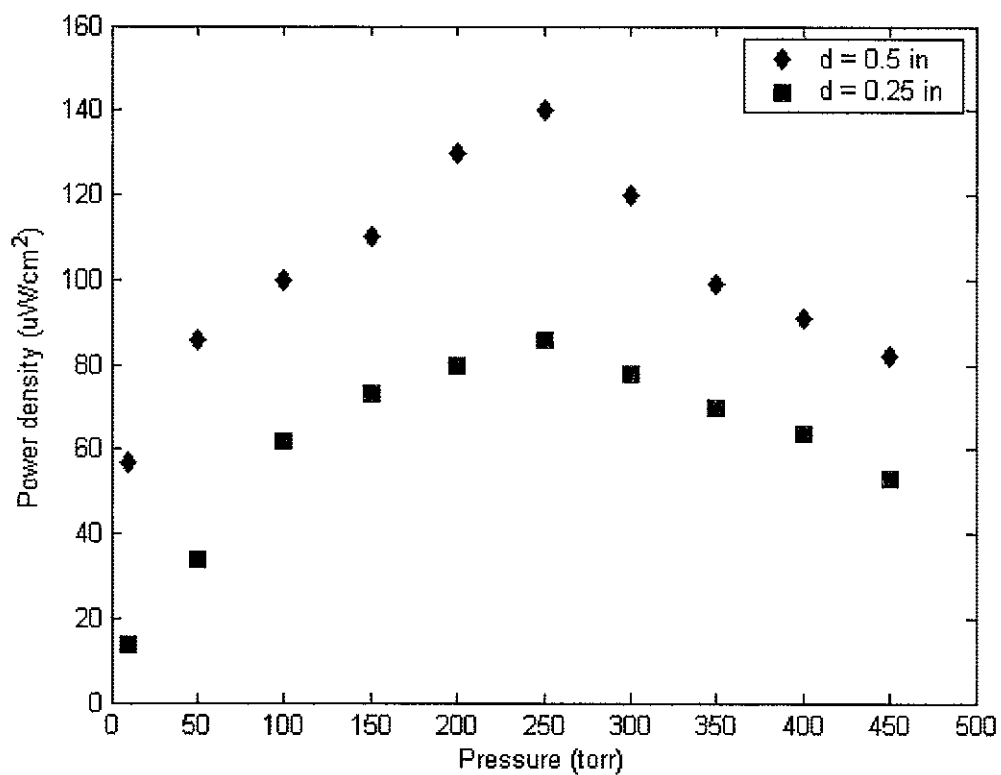


Fig. 4.18. Power density of the discharge as a function of Pressure at $V = 16$ kV, $f = 18$ kHz for discharge tube diameters of 0.25 and 0.5 inch. UV photometer is placed 2-inch from source.

Fig. 4.19. The efficiency of the lamp with large discharge tube diameter ($d = 0.5$ in) showed similar pressure dependence as that of the one with small discharge tube diameter ($d = 0.25$ in). The efficiency increased until it reaches a pressure of 250 torr and then decreased with increase in pressure. At all pressures, the efficiency achieved by the lamp with the large discharge tube diameter is greater than that of the small discharge tube diameter. The efficiency versus pressure (Fig. 4.19) resembles the power density versus pressure plot (Fig. 4.18). This is because the power consumed by the lamp doesn't vary too much with pressure (see Fig. 4.5).

The efficiency versus power for both discharge tube diameters is shown in Fig 4.20. The efficiency of the lamp with large discharge tube diameter ($d = 0.5$ in) showed similar power dependence as that of the lamp with small discharge tube diameter ($d = 0.25$ in). The conversion efficiency decreased with increase in the power consumed by the lamp. With the same input electrical power, high efficiency can be achieved by using a large discharge tube diameter.

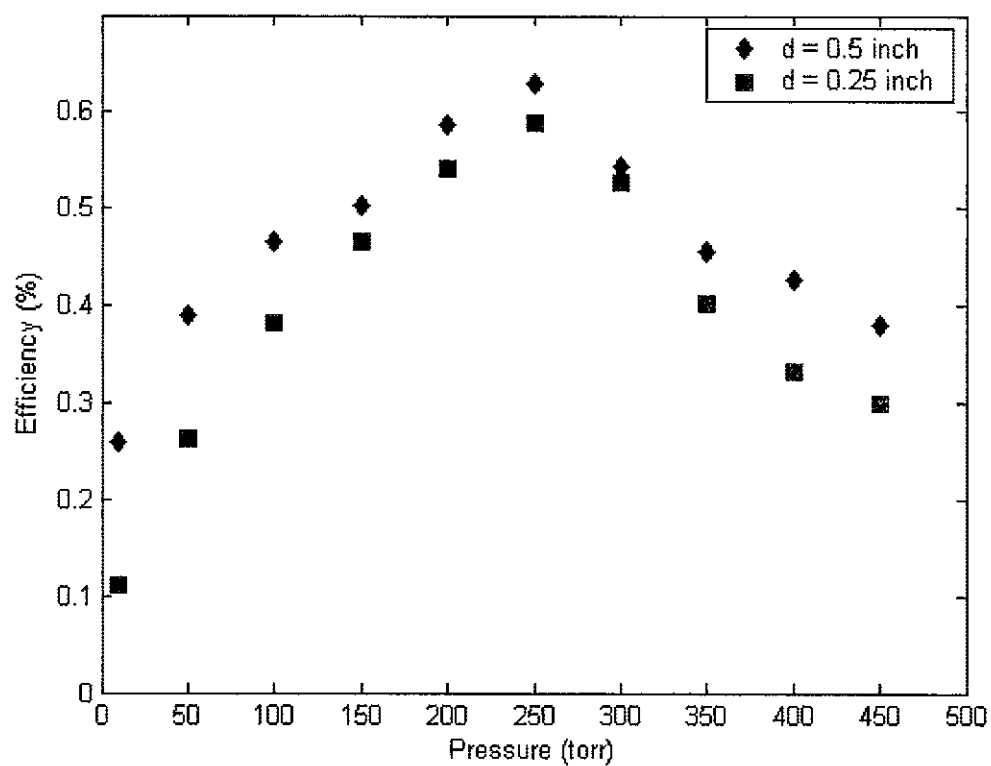


Fig. 4.19. Efficiency as a function of Pressure for discharge tube diameters of 0.25 and 0.5 inch: $f = 18$ kHz, $V = 16$ kV.

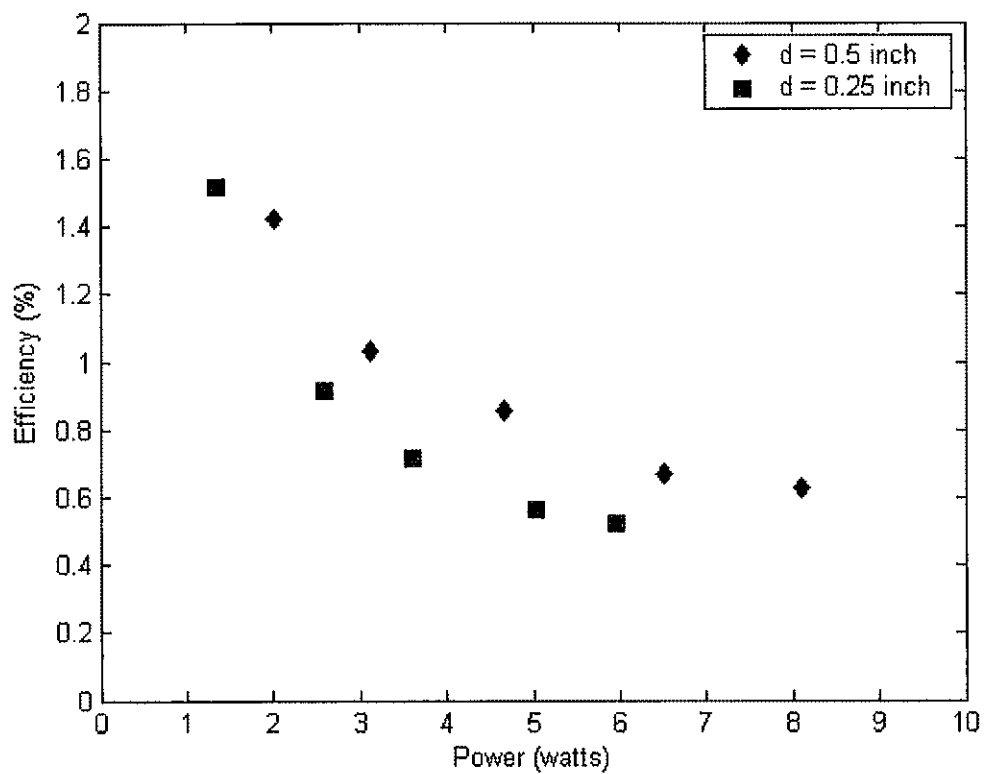


Fig. 4.20. Efficiency as a function of Power for discharge tube diameters of 0.25 and 0.5 inch: $f = 18$ kHz, $p = 250$ torr.

CHAPTER V

SUMMARY

An intense UV excimer source that emits radiation in the 200 to 280 nm spectral range has been successfully developed. The operation of the excimer UV source depends on the decomposition of the excimers that are formed in a non-equilibrium discharge. For efficient formation of excimers, two conditions must be satisfied. High-energy electrons, whose energy is high enough to excite the atoms in the ground state, must be present in the discharge. Secondly the pressure in the discharge tube must be relatively high, between 0.1 to one atmospheres, to make the three body reactions that are responsible for the formation of excimers more favorable. Non-equilibrium discharges can provide high-energy electrons and can operate at high pressures, which are required for the formation of excimers. So, a cylindrical dielectric barrier discharge (C-DBD), which is a non-equilibrium discharge, is used in our experiments to generate the excimer UV radiation.

The electrode geometry used in our system is very simple. A copper strap, which is wrapped outside the discharge tube and two stainless steel rings connected at the ends of the discharge tube act as electrodes. The discharge tube used is cylindrical in shape and is made up of quartz to allow the UV radiation to pass through. Also quartz is a dielectric material and so the discharge tube itself acts as a dielectric barrier, which is necessary in a DBD. The production of plasma requires a voltage of several kilovolts at frequencies in the kHz range to excite the gas in the discharge tube. So, a kHz amplifier along with a high voltage transformer that gives an output of up to 20 kilovolts is used. A discharge is generated inside the tube when an AC voltage of several kilovolts, at a frequency of few kilohertz, is applied between the electrodes.

Our objective is to generate intense excimer UV radiation in the wavelength range of 200 to 280 nm. For this purpose a gas mixture of krypton and chlorine with a buffer gas of neon is selected. KrCl^* , Cl_2^* and Cl_2^{**} emission bands (in the 200 to 280nm range) are formed as a result of the discharge in the Ne/Kr/ Cl_2 gas mixture. The discharge in a research grade gas mixture of Neon (89.9%), Krypton (10%) and Chlorine (0.1%) is studied extensively. The discharge in this gas mixture is shown to be an efficient UV source in the wavelength range of 200 to 280 nm. The emission in this range is because of the presence of KrCl^* , Cl_2^* and Cl_2^{**} excimers in the discharge. As the excimers are highly unstable, they disintegrate giving up the extra energy in them in the form of UV photons.

The emission spectrum of the discharge in Ne/Kr/ Cl_2 gas mixture in the wavelength range of 180 to 350 nm is observed. The discharge is found to have strong emission bands centered around 200 nm (Cl_2^{**}), 222 nm (KrCl^*), 258 nm (Cl_2^*) and 325 ± 15 nm (Kr_2Cl^*). Emission spectra for different combinations of pressure in the discharge, discharge tube diameter, input voltage and frequency are observed. In all these experiments, our main focus is on how to increase the intensity of UV radiation in the wavelength range of 200 to 280 nm. To achieve this objective, the dependence of the UV radiation intensity on four operating parameters is studied using spectrometer and UV calibrated photometer. The intensity of the UV radiation increased with increase in the pressure/frequency until it reaches a maximum value, after that the intensity decreased. The maximum UV radiation intensity is achieved at a pressure of 250 torr and frequency of 18 kHz. The UV radiation intensity is found to be an increasing function of the other two operating parameters: input voltage and discharge tube diameter.

The electrical power consumed by the discharge is calculated from the Q-V graph using the lissajous method. The effect of pressure, discharge tube diameter, input voltage and frequency on the power consumed by the lamp is studied. The pressure in the discharge showed no affect on the power consumed by the lamp. But an increase in either discharge tube diameter or input voltage or frequency showed an increase in the power consumed by the lamp. The power density of the UV radiation emitted from the lamp under different operating conditions is measured using a photometer. A maximum power density of 140 microwatts is measured at a distance of 2 inch from the discharge tube. At the same distance, the power density of the radiation emitted by the commercial lamp is only 50 microwatts. The conversion efficiency of the lamp varied depending on pressure in the discharge and power consumed by the lamp. Efficiencies as high as 1.5% can be achieved under optimal conditions. This low cost excimer lamp can be used in applications like surface modification and water treatment.

REFERENCES

1. Perspectives on plasmas website, <http://www.plasmas.org/basics.htm> and <http://www.plasmas.org/powers.htm>.
2. Ch.K. Rhodes (ed.), Topics in Applied Physics: Excimer Lasers **30**, Springer-Verlag, New York, 1984.
3. H. Kumagai, M. Obara, Appl. Phys. Lett. **54**, 2619 (1989).
4. D. Lindau, H.F. Dobeles, Rev. Sci. Instrum. **59**, 565 (1988).
5. A.K. Shuaibov, A.I. Dashchenko, I.V. Shevera, High Temp. **40**, 309 (2002).
6. M. Moselhy, I. Petzenhauser, K. Frank, K.H. Schoenbach, J. Phys. D: Appl. Phys. **36**, 2922 (2003).
7. K.H. Schoenbach, M. Moselhy, W. Shi, R. Bentley, J. Vac. Sci. Technol. A **21**, 1260 (2003).
8. K. Mitsuhashi, T. Igarashi, M. Komori, T. Takada, E. Futagami, J. Kawanaka, S. Kubodera, K. Kurosawa, W. Sasaki, Opt. Lett. **20**, 2423 (1995).
9. U. Kogelschatz, Pure and Appl. Chem. **62**, 1667 (1990).
10. Z. Falkenstein and J.J. Coogan, J. Phys. D: Appl. Phys. **30**, 2704 (1997).
11. I.W. Boyd, J.Y. Zhang, P. Bergonzo, Proceedings of SPIE **2403**, 290 (1995).
12. J.Y. Zhang, I.W. Boyd, J. Appl. Phys **80**, 633 (1996).
13. B. Gellert, U. Kogelschatz, Appl. Phys. B: Lasers and Optics **52**, 14 (1991).
14. B. Eliasson, U. Kogelschatz, Appl. Phys. B: Lasers and Optics **46**, 299 (1988).
15. R. Hippler, S. Pfau, M. Schmidt, and K.H. Schoenbach, Low temperature plasma physics: Fundamental aspects and applications, 1st edition, WILEY-VCH, 2001.
16. B. Eliasson, W. Egli and U. Kogelschatz, Pure and Appl. Chem. **66**, 1275 (1994).

17. Ahmed El-Habachi, Ph.D. thesis, Old Dominion University, Norfolk, 1998.
18. M. Moselhy, Ph.D. thesis, Old Dominion University, Norfolk, 2002.
19. U. Kogelschatz, B. Eliasson and W. Egli, *Pure and Appl. Chem.* **71**, 1819 (1999).
20. B. Eliasson, U. Kogelschatz, *IEEE Trans. Plasma Sci.* **19**, 309 (1991).
21. U. Kogelschatz, *Plasma Chemistry and Plasma Processing*, **23**, 1 (2003).
22. U. Kogelschatz, H. Esrom, J.Y. Zhang, I.W. Boyd, *Appl. Surf. Sci.* **168**, 29 (2000).
23. M. Laroussi, "The Electrodeless Discharge at Atmospheric Pressure", *IEEE Int. Conf. Plasma Sci.*, Monterey, CA, p.203, 1999.
24. M. Laroussi, "Electrodeless Excimer UV Lamp", US patent 6,858,988, (2005).
25. U. Kogelschatz, *Appl. Surf. Sci.* **54**, 410 (1992).
26. U. Kogelschatz, *Proceedings of SPIE* **5483**, 272 (2004).
27. T. Textor, T. Bahners, E. Schollmeyer, *J. Industrial Textiles* **32**, 279 (2003).
28. D. Praschak, T. Bahners, E. Schollmeyer, *Appl. Phys. A* **66**, 69 (1998).
29. A. K. Shuaibov, L. L. Shimon, and I. A. Grabovaya, *Tech. Phys. Lett.* **29**, 871 (2003).
30. V.F. Tarasenko, *Pure Appl. Chem.* **74**, 465 (2002).
31. C.W. Werner, E.V. George, P.W. Hoff, and Ch.K. Rhodes, *IEEE J. Quantum Electronics* **13**, 769 (1977).
32. P. Moutard, P.Laporte, J.L. Subtil, N. Damany, and H. Damany, *J. Chem. Phys.* **88**, 7485 (1988).
33. I.W. Boyd, J.Y. Zhang, *Solid State Electronics*, **45**, 1413 (2001).

34. V.E. Peet, E.V.Slivinskii, A.B.Treshchalov, *Sov.J.Quantum Electron* **20**, 372 (1990).
35. K.Nakamura, *J. Appl. Phys.* **83**, 1840 (1988).
36. A.N. Panchenko, V.F. Tarasenko, *IEEE J. Quantum Electronics* **31**, 1231 (1995).
37. R.C.Sze, *IEEE J. Quantum Electronics*, **QE-15**, 1338 (1979).
38. J.E. Velazco, J. H. Kolts, and D. W. Setser, *J. Chem. Phys.* **65**, 3468 (1976).
39. M. Tsuji, M. Furusawa, H. Kouno, Y. Nishimura, *J.Chem. Phys.* **94**, 4291 (1991).
40. J.B. Nee, *Chinese journal of physics* **29**, 553 (1991).
41. M.I. Lomaev, V.S. Skakun, E.A. Sosnin, V.F. Tarasenko, D.V. Shifts, M.V. Erofeev, *Physics Uspekhi* **46**, 193 (2003).
42. P. Bergonzo, I.W. Boyd, *J. Appl. Phys* **76**, 4372 (1994).
43. M. Laroussi, F.C. Dobbs, Z. Wei, M.A. Doblin, L.G. Ball, K.R. Moreira, F.F. Dyer, J.P. Richardson, *IEEE transactions of plasma science*, **30**, 1501 (2002).
44. Z. Falkenstein, *Development of an excimer UV light source system for water treatment*, Ushio America, Inc., 2001.
45. J.Y. Zhang, G. Windall, I.W. Boyd, *Appl. Surf. Sci.* **186**, 568 (2002).
46. http://www.pgo-online.com/intl/katalog/curves/quartz_glass_transmission.html
47. *SpectroPro 500i manual*, Acton Research Corporation.
48. A.K. Shuaibov, A.I. Dashchenko, L.L. Shimon, I.V. Shevera, *Tech. Phys. Lett.* **28**, 702 (2002).

VITA
Sudhakar Reddy Alla

DEGREES:

Master of Science in Electrical Engineering, Old Dominion University, Norfolk, Virginia, USA, December 2006.

Bachelor of Technology in Electrical Engineering, JNTU, Anantapur, AP, India, May 2004.

PROFESSIONAL CHRONOLOGY:

Department of Electrical Engineering, Old Dominion University, Norfolk, Virginia.

Graduate Research Assistant, June 2005 – December 2006.

PUBLICATIONS:

M. Laroussi, C. Tendero, X. Lu, S. Alla, W.L. Hynes, “ Inactivation of Bacteria by the Plasma Pencil”, *Plasma Process. Polym.* **3**, 470 (2006).